scientific reports

Check for updates

OPEN

The high adsorption performance of banana (*Musa* ABB Cv. Kluai 'Namwa') beaded materials modified with zinc and magnesium oxides for cadmium removal

Pornsawai Praipipat[1,2]✉, Pimploy Ngamsurach[1,2], Yada Khamenthong[1] & Niraya Himlee[1]

Wastewater contaminated with cadmium is a concern because of its toxicity, persistence, and bioaccumulation to the environment, ecosystem, and human health, so it is required to remove cadmium(II) ions before releasing them to receiving water. Banana powder beads (BPB), banana powder doped ZnO beads (BPZB), banana powder doped MgO beads (BPMB), and banana powder doped ZnO + MgO beads (BPZMB) were synthesized as the novel cadmium adsorbents, and their characterizations, cadmium adsorption performances, cadmium adsorption patterns and mechanisms, thermodynamic study, and reusability were investigated. BPMB had the highest specific surface area of 16.60 m^2/g and the smallest pore size of 1.69 nm than other materials. BPB was an amorphous structure, whereas BPZB, BPMB, and BPZMB were crystalline structures presenting their specific metal oxide peaks of ZnO or MgO. They were coarse surfaces and had a spherical shape consisting of C, O, Ca, Cl, and Na. Their main functional groups were O–H, C–H, C=O, C–O, and N–H. The points of zero charge of BPB, BPZB, BPMB, and BPZMB were 5.37, 6.75, 9.87, and 9.43. The cadmium removal efficiencies of BPB, BPZB, BPMB, and BPZMB were 89.18%, 96.62%, 99.59%, and 97.85%, and their q_m values were 90.09, 232.56, 454.55, and 303.03 mg/g, respectively. Thus, the metal oxide helped to improve material efficiency, especially MgO. The Freundlich and pseudo-second-order kinetic models were good fit models for describing their adsorption patterns and mechanisms. The increasing temperature affected to decrease their cadmium adsorptions. They could be reused in more than 3 cycles of more than 73% of cadmium adsorption. The electrostatic interaction played an important role in describing their cadmium adsorptions. Therefore, BPBM was a good cadmium adsorbent for application in industrial wastewater treatment since it had a higher performance of cadmium adsorption than other materials.

Keywords Fruit waste, Metal oxide, Adsorption, Heavy metal, Reusability

The toxicities of heavy metals are generally known to affect many human health effects of main function disorders and many human diseases. The high-risk effect depends on the type of heavy metals which mercury, cadmium, and lead are the top three highly dangerous heavy metals with high toxicities causing human carcinogenesis. Many industries of battery, metal plating, steel, dyes, pigments, pharmaceutical products, and ceramics use cadmium in their manufacturing processes, so their wastewater may have cadmium contamination. Thus, they need to be eliminated before releasing to receiving water. The United States Environmental Protection Agency (USEPA) is also required to treat cadmium-contaminated wastewater to be below 0.005 mg/L for drinking water, and the World Health Organization (WHO) is recommended not to exceed 0.03 mg/L in wastewater[1].

Many previous studies popularly used the adsorption method for several heavy metal removals more than other methods of chemical precipitation, electrodialysis, ion exchange, membrane separation, photocatalysis, and nanotechnology because it is an effective method, easy operation, low energy requirement, many options of adsorbents, and reasonable operation cost. Many options of adsorbents might be from agriculture, industry,

[1]Department of Environmental Science, Faculty of Science, Khon Kaen University, Khon Kaen 40002, Thailand. [2]Environmental Applications of Recycled and Natural Materials (EARN) Laboratory, Khon Kaen University, Khon Kaen 40002, Thailand. ✉email: pornprai@kku.ac.th

and waste for eliminating target pollutants. Among those adsorbents, waste adsorbents are interesting because they can adsorb many heavy metals and save operating costs. Moreover, they are a good way of waste recycling to offer waste-sustainable uses. Many waste adsorbents from industry, agriculture, animal, vegetable, and fruit for heavy metal removals are illustrated in Table 1. Among those adsorbents, fruit wastes are interesting because they can adsorb various heavy metals and reduce a large amount of waste from human consumption resulting in good waste management. Especially, banana is a popular human fruit around the world resulting in an abundant amount of banana peels. Since they have good chemical compositions of cellulose, hemicellulose, pectin, and lignin, they are used for eliminating pollutants in wastewater in many previous studies in Table 1.

Several methods by thermal, alkaline, acid, and metal oxide modifications have been studied in many previous studies to improve the material efficiency of fruit peels for target heavy metals shown in Table 2. The thermal method used a temperature from 200 to 550 °C to prepare pomelo, banana, and mango peels to be biochar for adsorbing copper(II) and cadmium(II) ions[2–4]. For the alkaline method, sodium hydroxide (NaOH) was used for activating melon and lemon peels to remove copper(II), cadmium(II), and nickel(II) ions[5,6]. For the acid treatment, phosphoric acid (H_3PO_4) and hydrochloric acid (HCl) were applied to activate banana peels to adsorb cadmium(II) and chromium(VI) ions[7,8]. For the metal oxide modifications, metal oxides of iron(II, III) oxide (Fe_3O_4), titanium dioxide (TiO_2), aluminum oxide (Al_2O_3), and magnesium oxide (MgO) were used to modify pomelo, pomegranate, banana, and watermelon peels for eliminating lead(II), copper(II), arsenic(III), and cadmium(II) ions[2,9–11]. Among those methods, the addition of metal oxide into fruit peels gave a higher adsorption capacity (q_m) than other methods. As a result, this method is an interesting use to improve material efficiency for heavy metal removals. For banana peels, they were modified by thermal, acid, and aluminum oxide (Al_2O_3) in a powder form for removing lead(II) ions[7,12,13], and they were also modified by acid and Al_2O_3 in a powder form for adsorbing cadmium(II) and chromium(VI) ions[7,8,13]. However, no one used zinc oxide (ZnO) or magnesium oxide (MgO) for modifying banana peels in a bead form to remove cadmium(II) ions in aqueous solution, so it was a research gap to develop a low-cost adsorbent from banana peels as a novel cadmium adsorbent. Therefore, this study was the first attempt to synthesize novel cadmium adsorbents from

Waste adsorbents	Heavy metals	Dose (g)	Time (min)	Temp. (°C)	pH	Conc. (mg/L)	Volume (mL)	q_m (mg/g)	References
Industrial									
Sawdust	Pb(II)	2	300	25	5	30–70	200	11.74	[14]
Fly ash	Pb(II)	0.04	60	23	3.8	2.5–20	20	51.98	[15]
Red mud	Cd(II)	0.01	1440	20	6	200	20	32.18	[16]
Steel slag	Pb(II)	0.4	1440	25	7	46–598	50	59.81	[17]
Steel slag	Cu(II)	0.4	1440	25	7	46–598	50	4.98	[17]
Agricultural									
Sugarcane bagasse	Pb(II)	0.6	360	25	5	5–30	200	6.16	[18]
Wheat bran	Pt(IV)	0.5	1440	25	-	50	500	4.64	[19]
Animal									
Chicken eggshell	Pb(II)	0.5	240	25	5	10–70	200	25.19	[20]
Duck eggshell	Pb(II)	3	240	25	5	10–70	200	4.66	[21]
Vegetable									
Potato peel	Cr(II)	2	60	22	-	5-500	50	11.10	[22]
Potato peel	Pb(II)	2	60	22	-	5-500	50	12.50	[22]
Fruit									
Lemon peel	Pb(II)	4	360	25	5	10–70	100	1.81	[23]
Orange peel	Pb(II)	4	360	25	5	10–70	100	1.88	[24]
Orange peel	Pb(II)	2	60	22	-	5-500	50	25.00	[22]
Orange peel	Cr(II)	2	60	22	-	5-500	50	12.50	[22]
Pomelo peel	Pb(II)	0.1	120	30	5.5	50–200	50	47.18	[25]
Pomelo peel	Cd(II)	0.1	100	30	5.5	10–50	50	13.35	[25]
Watermelon peel	Pb(II)	0.25	20	30	2	60–120	15	10.10	[26]
Watermelon peel	Fe(II)	0.25	20	30	2	60–120	15	7.25	[26]
Passion fruit peel	Pb(II)	0.5	60	22	-	5-500	50	20.00	[22]
Passion fruit peel	Cr(II)	0.5	60	22	-	5-500	50	3.30	[22]
Banana peel	Cu(II)	2	90	25	5	40–120	100	3.29	[27]
Banana peel	Cu(II)	1	-	-	5.5	10–100	1000	28.56	[28]
Banana peel	Cu(II)	1	60	30	5	100–1000	50	61.73	[29]
Banana peel	Pb(II)	1	-	-	5.5	10–100	1000	66.67	[28]
Banana peel	Zn(II)	1.5	60	30	5	100–1000	50	55.56	[29]

Table 1. Waste adsorbents for eliminating heavy metals.

Modification methods	Fruit peels	Heavy metals	Dose (g)	Time (min)	Temp. (°C)	pH	Conc. (mg/L)	Volume (mL)	q_m (mg/g)	References
Thermals										
Biochar (pyrolysis at 550 °C)	Pomelo	Cu(II)	-	360	25	6	0-500	100	47.54	2
Hydrochar (200 °C)	Banana	Cd(II)	0.125	30	25	6	5-100	20	4.20	3
Hydrochar (250 °C)	Banana	Cd(II)	0.125	30	25	6	5-100	20	3.40	3
Biochar (500 °C)	Mango	Cd(II)	0.05	1,440	25	-	10–300	25	13.28	4
Alkalines										
Sodium hydroxide (NaOH)	Melon	Cu(II)	0.075	60	30	6.6	10–500	50	77.76	5
Sodium hydroxide (NaOH)	Melon	Cd(II)	0.075	60	30	6.6	10–500	50	76.16	5
Sodium hydroxide (NaOH)	Lemon	Ni(II)	0.125	180	25	5	5-500	25	36.74	6
Acids										
Phosphoric acid (H_3PO_4)	Banana (hydrocchar at 200 °C)	Cd(II)	0.04	1,440	-	6	3-150	40	94.52	7
Hydrochloric acid (HCl)	Banana	Cr(VI)	0.1	60	25	-	5-100	-	10.42	8
Metal oxides										
Iron(II, III) oxide (Fe_3O_4)	Pomelo (pyrolysis at 550 °C)	Pb(II)	-	360	25	5	0-500	100	205.39	2
	Pomelo (pyrolysis at 550 °C)	Cu(II)	-	360	25	6	0-500	100	81.91	2
Titanium dioxide (TiO_2)	Pomegranate	As(III)	0.025	1,440	25	7	10–600	25	76.92	9
Aluminum oxide (Al_2O_3)	Banana (calcined at 600 °C)	Cd(II)	0.1	40	-	6	20–100	20	43.00	13
	Banana (calcined at 600 °C)	Pb(II)	0.1	40	-	6	20–100	20	57.00	13
Magnesium oxide (MgO)	Watermelon (pyrolysis at 600 °C)	Pb(II)	0.1	1,440	-	-	46	20	558.00	11
	Watermelon (pyrolysis at 700 °C)	Pb(II)	0.1	1,440	-	-	46	20	724.00	11

Table 2. Acid, alkaline, thermal, and metal oxide modifications in fruit peels for heavy metal removals.

banana peels with or without modification of ZnO or MgO in a bead form to investigate how much ZnO or MgO increases banana material efficiency for cadmium adsorption. Moreover, the addition of one metal oxide (ZnO or MgO) or two metal oxides of ZnO + MgO into banana peel materials should be chosen for obtaining high cadmium adsorption. Furthermore, this study also presented a novel material form of cadmium adsorbents for easy separation after treatment which might be applied in industrial applications to save operation costs as well.

This study aimed to synthesize banana powder beads with ZnO or MgO modifications which were banana powder beads (BPB), banana powder doped ZnO beads (BPZB), banana powder doped MgO beads (BPMB), and banana powder doped ZnO + MgO beads (BPZMB) for cadmium removals in aqueous solution. Their physiochemical properties on specific surface area, pore volumes, and pore size, crystalline structures, surface morphologies, chemical compositions, functional groups, and points of zero charge were also studied by Brunauer-Emmett-Teller (BET), X-ray diffractometer (XRD), Field emission scanning electron microscopy and focus ion beam (FESEM-FIB) with energy dispersive X-ray spectrometer (EDX), and Fourier transform infrared spectroscopy (FT-IR). Moreover, their cadmium removal efficiencies were investigated by a series of batch experiments, adsorption isotherms, and kinetics. The temperature effects on their cadmium removals were also explored by the thermodynamic study, and the desorption experiments were used for studying the material reusability.

Materials and methods

Raw material preparation

Musa ABB cv. Kluai 'Namwa' peels were obtained from a fried banana shop in Khon Kaen province, Thailand. They were washed with tap water to eliminate the contaminants, and then they were dried in a hot air oven (Binder, FED 53, Germany) at 80 °C overnight. After that, they were blended and sieved in size of 125 µm. Finally, they were kept in a desiccator before use called banana powder (BP)[20,30].

Chemicals

The chemicals used in this study were an analytical grade used without purification, and the details were demonstrated in the supplementary material.

Banana material synthesis

Banana material synthesis consisted of two steps which were banana powder modifications by zinc oxide (ZnO) or magnesium oxide (MgO) and banana bead materials with or without metal modifications which modified an idea from the studies of Praipipat, P et al.[31,30]. The schematic flow diagram of banana material synthesis is demonstrated in Fig. 1 and the details were clearly described in the supplementary material.

Material characterizations

The material characterizations of BPB, BPZB, BPMB, and BPZMB were investigated with several characterized equipment, and the details are demonstrated in Table 3.

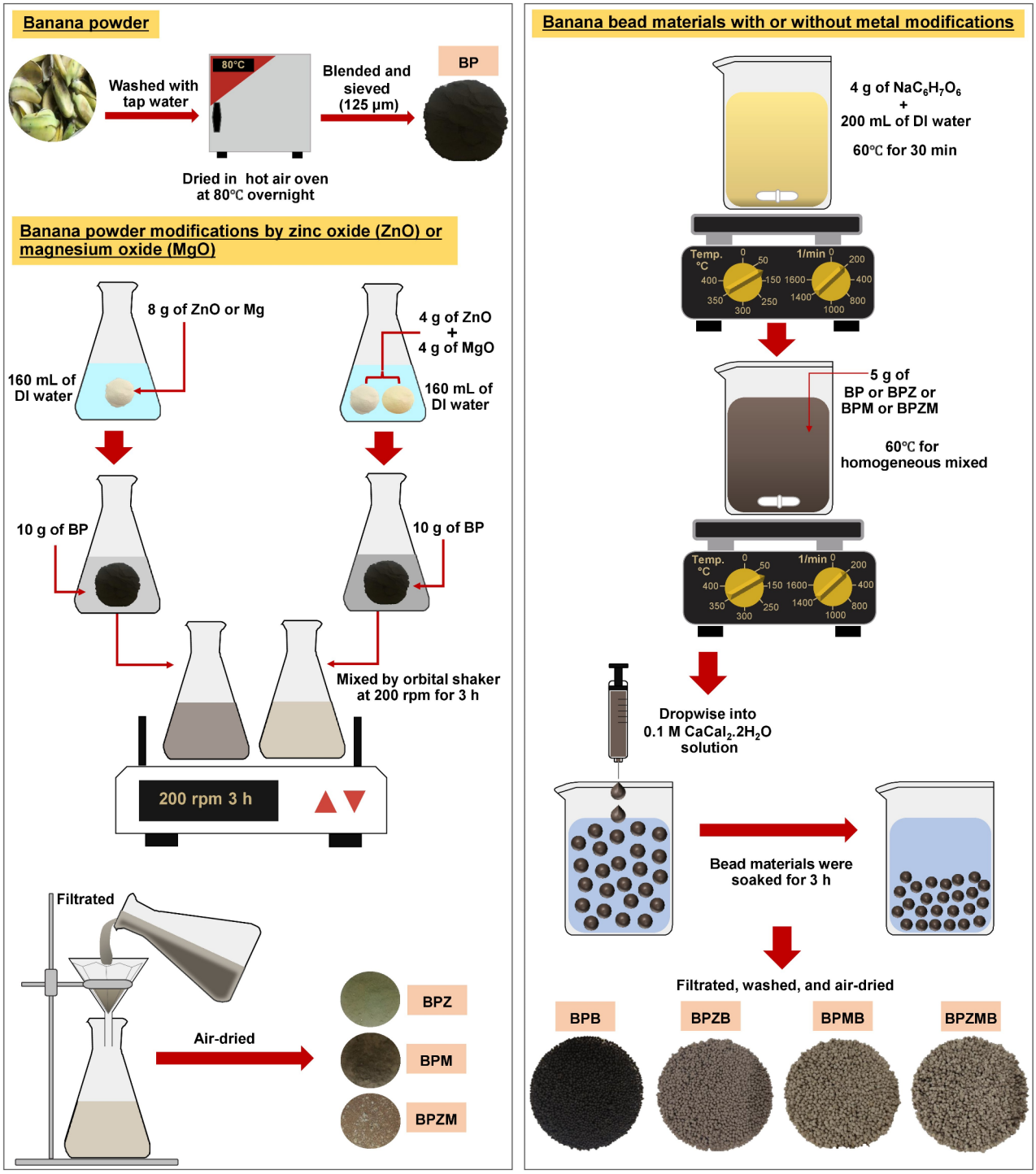

Fig. 1. The schematic flow diagram of banana material synthesis for banana powder beads (BPB), banana powder doped ZnO beads (BPZB), banana powder doped MgO beads (BPMB), and banana powder doped ZnO + MgO beads (BPZMB).

The points of zero charge

The points of zero charge (pH_{pzc}) of BPB, BPZB, BPMB, and BPZMB were studied following the method of Praipipat et al.[31] by using 50 mL of 0.1 M NaCl solutions at pH 1–12 and 0.1 g of material with shaking at 150 rpm for 24 h. After that, the final pH solution was measured by a pH meter (Mettler Toledo, Seven2Go pH with InLab Expert Go-ISM, Switzerland) and the graph of ΔpH ($pH_{final} - pH_{initial}$) versus $pH_{initial}$ was plotted to determine pH_{pzc}.

Material characterizations	Equipments
Specific surface area, pore volume, and pore size	Brunauer-Emmett-Teller (BET) (QUADRASORB evo, Austria) with N_2 adsorption-desorption isotherm at 77.35 K and degas temperature of 80 °C for 7 h
Crystalline structure	X-ray diffractometer (XRD) (Bruker, D8 Advance, Switzerland) with 2Θ of 5–80°
Surface morphology and chemical composition	Field emission scanning electron microscopy and focus ion beam (FESEM-FIB) with energy dispersive X-ray spectrometer (EDX) (FEI, Helios NanoLab G3 CX, USA) by using 10 kV measurement at the magnification of 100X with 1 mm and 1,500X with 100 µm
Chemical functional group	Fourier transform infrared spectroscopy (FT-IR) (Bruker, TENSOR27, Hong Kong) at the wavenumber of 4000–600 cm^{-1} with a resolution of 4 cm^{-1} and 32 scans

Table 3. The details of material characterizations.

Models	Parameters	Refs
Isotherms		
Langmuir Linear: $C_e/q_e = 1/q_m K_L + C_e/q_m$ Nonlinear: $q_e = q_m K_L C_e/1 + K_L C_e$	C_e = The equilibrium of cadmium concentration (mg/L) q_e or q_m = The adsorption capacity or maximum adsorption capacity of cadmium on material at equilibrium (mg/g) K_L = Langmuir constant (L/mg)	32
Freundlich Linear: $\log q_e = \log K_F + 1/n \log C_e$ Nonlinear: $q_e = K_F C_e^{1/n}$	K_F = Freundlich constant (mg/g)(L/mg)$^{1/n}$ n = The adsorption intensity	33
Temkin Linear: $q_e = RT/b_T \ln A_T + RT/b_T \ln C_e$ Nonlinear: $q_e = RT/b_T \ln A_T C_e$	R = The universal gas constant (8.314 J/mol) T = The absolute temperature (K) b_T = The constant related to the heat of adsorption (J/mol) A_T = The equilibrium binding constant corresponding to maximum binding energy (L/mg)	34
Dubinin-Radushkevich Linear: $\ln q_e = \ln q_m - K_{DR}\varepsilon^2$ Nonlinear: $q_e = q_m \exp(-K_{DR}\varepsilon^2)$	K_{DR} = The activity coefficient related to mean adsorption energy (mol^2/J^2) ε = The Polanyi potential (J/mol)	35
Kinetics		
Pseudo-first-order Linear: $\ln(q_e - q_t) = \ln q_e - k_1 t$ Nonlinear: $q_t = q_e(1 - e^{-k_1 t})$	q_t = The adsorption capacity of cadmium on adsorbent material at the time (t) (mg/g). k_1 = Pseudo-first-order rate constant (1/min)	36
Pseudo-second-order Linear: $t/q_t = 1/k_2 q_e^2 + (t/q_e)$ Nonlinear: $q_t = k_2 q_e^2 t/(1 + q_e k_2 t)$	k_2 = Pseudo-second-order rate constant (g/mg·min)	37
Elovich Linear: $q_t = 1/\beta \ln \alpha\beta + 1/\beta \ln t$ Nonlinear: $q_t = \beta \ln t + \beta \ln \alpha$	α = The initial adsorption rate (mg/g/min) β = The extent of surface coverage (g/mg)	38
Intraparticle diffusion Linear and Nonlinear: $q_t = k_i t^{0.5} + C_i$	k_i = The intraparticle diffusion rate constant (mg/g·min$^{0.5}$) C_i = The constant that gives an idea about the thickness of the boundary layer (mg/g)	39

Table 4. Adsorption isotherm and kinetic models.

A series of batch experiments

The material dosage (0.02–0.5 g), contact time (1–12 h), temperature (20–50 °C), pH (3–10), and initial concentration (25–200 mg/L) of BPB, BPZB, BPMB, and BPZMB were examined by a series of batch experiments. The cadmium concentration of 100 mg/L, 100 mL of sample volume, and shaking speed of 150 rpm were applied as the control condition, and the triplicate samples were used to confirm the results. The optimum condition was chosen from the lowest value of each affecting factor obtaining the highest cadmium removal efficiency, and it was used for the next affecting factor. The atomic absorption spectrophotometry (AAS) (PerkinElmer, PinAAcle 900 F, USA) was used to measure the cadmium concentration. Cadmium removal efficiency (%) and the cadmium adsorption capacity (q_e) (mg/g) were calculated by Eqs. (1) and (2), respectively.

$$\text{Cadmium removal efficiency } (\%) = (C_0 - C_e)/C_0 \times 100 \quad (1)$$

where C_0 is the initial cadmium concentration (mg/L), and C_e is the final cadmium concentration (mg/L).

$$\text{The cadmium adsorption capacity } (q_e) = ((C_0 - C_e) \times V/M) \quad (2)$$

where V is the sample volume (L), and M is the mass of material (g).

Adsorption isotherms and kinetics

The details of adsorption isotherm and kinetic models used in this study to determine the adsorption patterns or mechanisms of BPB, BPZB, BPMB, and BPZMB are illustrated in Table 4.

For the adsorption isotherms, 0.2 g of BPB or 0.08 g of BPZB or 0.04 g of BPMB, or 0.06 g of BPZMB was added into 250 mL of Erlenmeyer flask containing 100 mL of different cadmium concentrations from 25 to 200 mg/L, pH 5, and tested the cadmium adsorption by an incubator shaker (New Brunswick, Innova 42, United

State) at 25 °C for BPZB and BPMB or 35 °C for BPB and BPZMB with a shaking speed of 150 rpm at 5 h for BPZB, BPMB, and BPZMB or 8 h for BPB.

For the adsorption kinetics, 2 g of BPB or 0.8 g of BPZB or 0.4 g of BPMB, or 0.6 g of BPZMB was added into 1000 mL of breaker containing 1000 mL of 100 mg/L of cadmium concentration, pH 5, and tested the cadmium adsorption by a jar test (JAR-TESTER, SF6, South Korea) with a shaking speed of 150 rpm for 12 h.

Thermodynamic study

Thermodynamic study was used to explore the temperature effect from 293.15 to 323.15 K on the cadmium removal efficiency of BPB, BPZB, BPMB, and BPZMB. The Eqs. (3)-(5) were used for calculating the thermodynamic parameters[40].

$$\Delta G^o = -RT \ln K_c \tag{3}$$

where R is the universal gas constant (8.314 J/mol K), T is the absolute temperature (K), and K_c is the equilibrium constant (L/mg).

$$\ln\ K_c = -\Delta H^o/RT + \Delta S^o/R \tag{4}$$

$$\Delta \mathrm{G}^o = \Delta H^o - T\Delta S^o \tag{5}$$

where ΔH° and ΔS° values are calculated from the slope and intercept of the linear graph between ln K_c ($K_c = q_e/C_e$) and $1/T$.

For the thermodynamic study, 0.2 g of BPB or 0.08 g of BPZB or 0.04 g of BPMB or 0.06 g of BPZMB was added to 250 mL of Erlenmeyer flask containing 100 mL of 100 mg/L cadmium concentration, pH 5, and tested the cadmium adsorption by an incubator shaker with different temperatures from 293.15 to 323.15 K with a shaking speed of 150 rpm at 5 h for BPZB, BPMB, and BPZMB or 8 h for BPB.

Material reusability

Material reusability of BPB, BPZB, BPMB, and BPZMB was examined by the desorption experiment following the method of Praipipat et al.[14] by using 0.5 M HNO_3 pushed out cadmium(II) ions from the saturated material with shaking at 150 rpm for 6 h, rinsed with deionized water, and air-dried before use in the next adsorption cycle. The cadmium desorption efficiency (%) is calculated by Eq. (6).

$$\text{Cadmium desorption efficiency } (\%) = (q_\mathrm{d}/q_\mathrm{a}) \times 100 \tag{6}$$

where q_d is the amount of cadmium desorbed (mg/L) and q_a is the amount of cadmium adsorbed (mg/L).

Result and discussion

The visual appearances of materials

The visual appearances of BPB, BPZB, BPMB, and BPZMB are shown in Fig. 2a-d which had a spherical shape with different colors with approximately 1 mm in size. BPB were black color beads, whereas BPZB were dark brown color beads. For BPMB and BPZMB, they were light brown color beads. Therefore, metal oxides of zinc and magnesium resulted in a change in the material color of banana beads.

Material characterizations

BET

The physicochemical properties on the specific surface area, pore volumes, and pore sizes of BPB, BPZB, BPMB, and BPZMB were determined by BET analysis and reported by the Barrett-Joyner-Halenda (BJH) adsorption method demonstrated in Table 5.

For the specific surface area, BPMB had a higher specific surface area of 16.60 m^2/g than other materials, so the addition of MgO affected the increase of the specific surface area of banana peel materials more than ZnO similar reported by the previous studies used MgO and ZnO to modify sugarcane bagasse and bagasse fly ash for adsorbing direct red 28 dye[41,42]. In addition, the pore volume results corresponded to the specific surface area that BPMB had the highest pore volume of 0.0388 cm^3/g. The pore size of BPMB was 1.69 nm which was smaller than other materials. Following the International Union of Pure and Applied Chemistry(IUPAC) classification, the sizes of material are classified as microporous size (< 2 nm) and mesoporous size (2–50 nm)[24]. Thus, BPB and BPZB were mesoporous materials, whereas BPMB and BPZMB were microporous materials. Since BPMB had the highest specific surface area and smallest pore size, it might have the ability to adsorb cadmium ions than other materials.

XRD

The crystalline structures of BPB, BPZB, BPMB, and BPZMB by XRD analysis are demonstrated in Fig. 3a-d. BPB was the amorphous structure shown in Fig. 3a whereas other materials displayed the crystal structures with presenting their metal oxide specifically peaks illustrated in Fig. 3b-d. For BPZB, it had the specific peaks of ZnO at the positions of 100, 002, 101, 102, 110, 103, 200, 112, 201, 004, and 202 (JCPDS no.36-1451) presented in Fig. 3b similar detected by previous studies used ZnO to modify bagasse, bagasse fly ash, chicken and duck eggshells for adsorbing reactive blue 4 dye[43,44]. For BPMB, it presented the specific peaks of MgO at the positions of 220, 111, 200, and 220 (JCPDS no.65–0476) demonstrated in Fig. 3c similar observed by a previous study that used MgO to load into biochar for removing lead(II) and cadmium(II) ions[45]. For BPZMB, it displayed the specific peaks of ZnO at the same positions with BPZB and MgO at the positions of 220, 111, and 220 which the

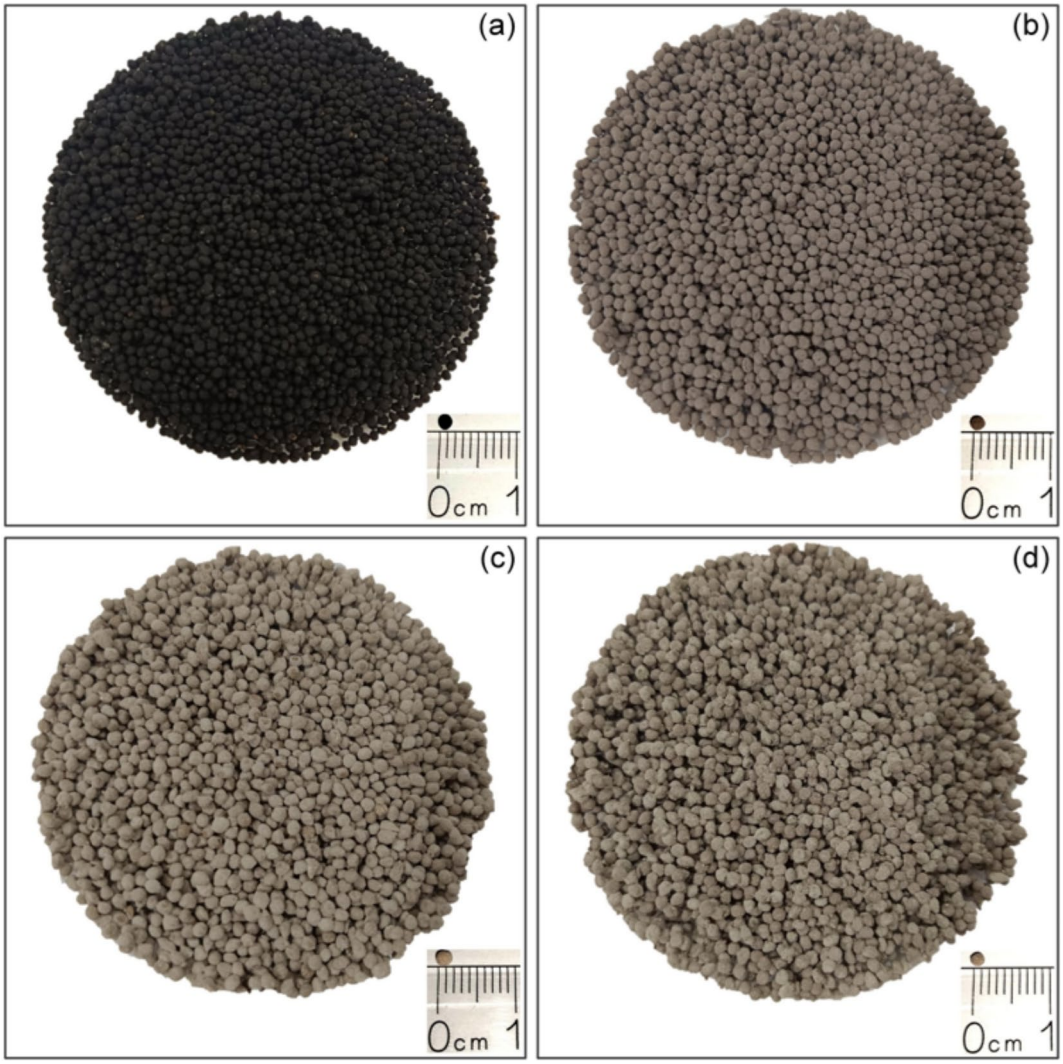

Fig. 2. The visual appearances of (a) BPB, (b) BPZB, (C) BPMB, and (d) BPZMB.

	Specific surface area (m^2/g)	Pore volume (cm^3/g)	Pore size (nm)
BPB	4.33	0.0087	2.77
BPZB	12.29	0.0336	2.16
BPMB	16.60	0.0388	1.69
BPZMB	15.13	0.0352	1.89

Table 5. The physiochemical properties on specific surface area, pore volumes, and pore sizes of BPB, BPZB, BPMB, and BPZMB.

ZnO dominated in BPZMB with higher intensity than MgO shown in Fig. 3d. Therefore, the results of the XRD analysis confirmed the successful addition of ZnO or MgO into banana peel materials.

FESEM-FIB and EDX

The surface morphologies of BPB, BPZB, BPMB, and BPZMB were analyzed by FESEM-FIB analysis, and the results are illustrated in Fig. 4a-h. For Fig. 4a-d, they demonstrated the beaded materials at the magnification of 100X with 1 mm which were coarse surfaces with having a spherical shape. For Fig. 4e-h, they displayed their surface morphologies by a cross-section at the magnification of 1,500X with 100 µm which were coarse and heterogeneous surfaces.

The chemical compositions of BPB, BPZB, BPMB, and BPZMB were analyzed by EDX analysis, and the results are illustrated in Table 6 reported in the percentage by weight (%wt). Carbon (C), oxygen (O), calcium (Ca), chlorine (Cl), and sodium (Na) were observed in BPB, BPZB, BPMB, and BPZMB which are generally

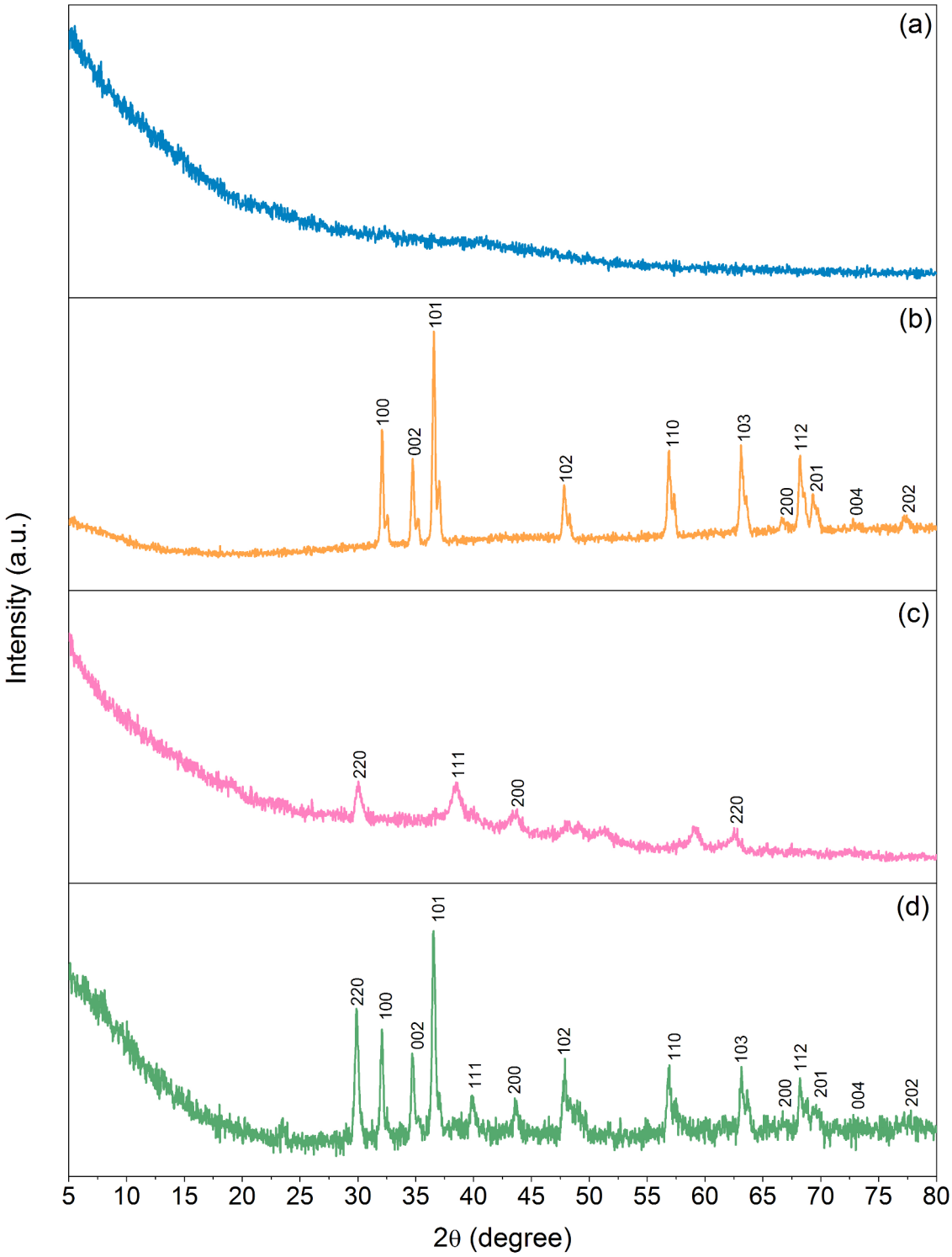

Fig. 3. The crystalline structures of (a) BPB, (b) BPZB, (C) BPMB, and (d) BPZMB.

found in fruit peels similar observed by previous studies[31,46]. In addition, Na, Ca, and Cl might form the chemicals of sodium alginate ($NaC_6H_7O_6$) and calcium chloride dihydrate ($CaCl_2.H_2O$) used for synthesizing bead materials. Furthermore, BPZB, BPMB, and BPZMB also detected zinc (Zn) or magnesium (Mg). The elemental distributions of BPZB, BPMB, and BPZMB shown in Fig. 4i-l could confirm the addition of ZnO or MgO into banana peel materials and found Zn or Mg distributions in BPZB, BPMB, and BPZMB.

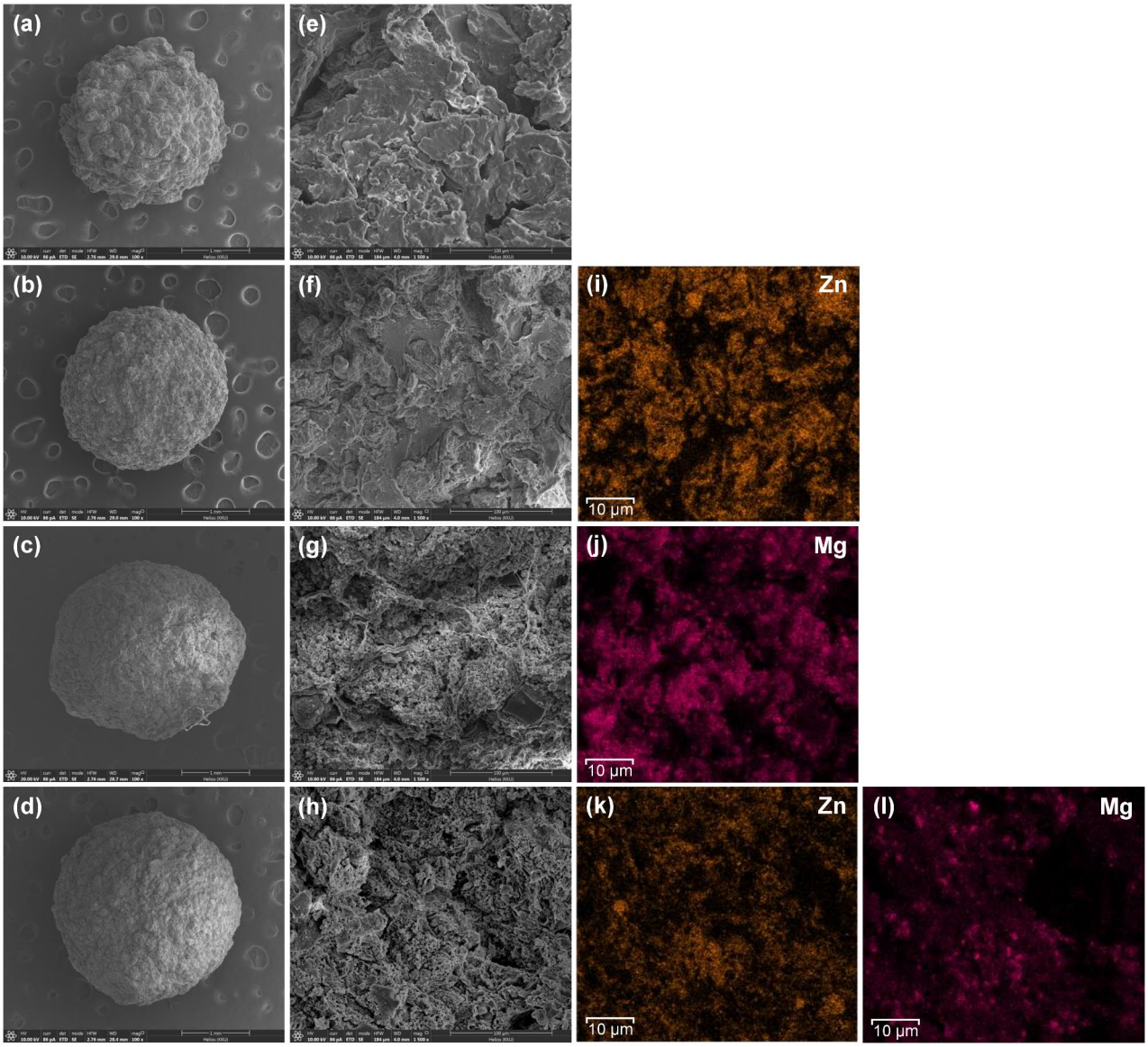

Fig. 4. The surface morphologies of (a and e) BPB, (b and f) BPZB, (c and g) BPMB, and (d and h) BPZMB, and the elemental distributions of(I) BPZB, (j) BPMB, and (k and l) BPZMB.

Chemical elements	The percentage by weight (%wt)			
	BPB	BPZB	BPMB	BPZMB
C	58.6	46.3	39.8	34.5
O	32.3	19.7	32.5	31.2
Ca	4.6	2.6	2.7	2.3
Cl	2.2	1.5	1.9	1.6
Na	2.3	2.1	2.4	2.0
Zn	-	27.8	-	14.6
Mg	-	-	20.7	13.8

Table 6. The chemical elements of BPB, BPZB, BPMB, and BPZMB.

FT-IR

The main chemical functional groups of BPB, BPZB, BPMB, and BPZMB identified by FT-IR analysis were O–H, C–H, C=O, C–O, and N–H. Moreover, the specific functional group of metal oxide with oxygen bond (Zn–O or Mg–O) was detected in BPZB or BPMB, or BPZMB found in a range of 600 cm^{-1}[142]. The results are demonstrated in Fig. 5a-d. For O–H, it represented the hydroxyl group with the stretching or bending vibrations observed in the ranges of 3200 and 1400 cm^{-1} generally found on pectin, cellulose, hemicellulose, and lignin in banana peels[47]. In addition, it presented the hydroxyl group with the stretching vibration in MgO

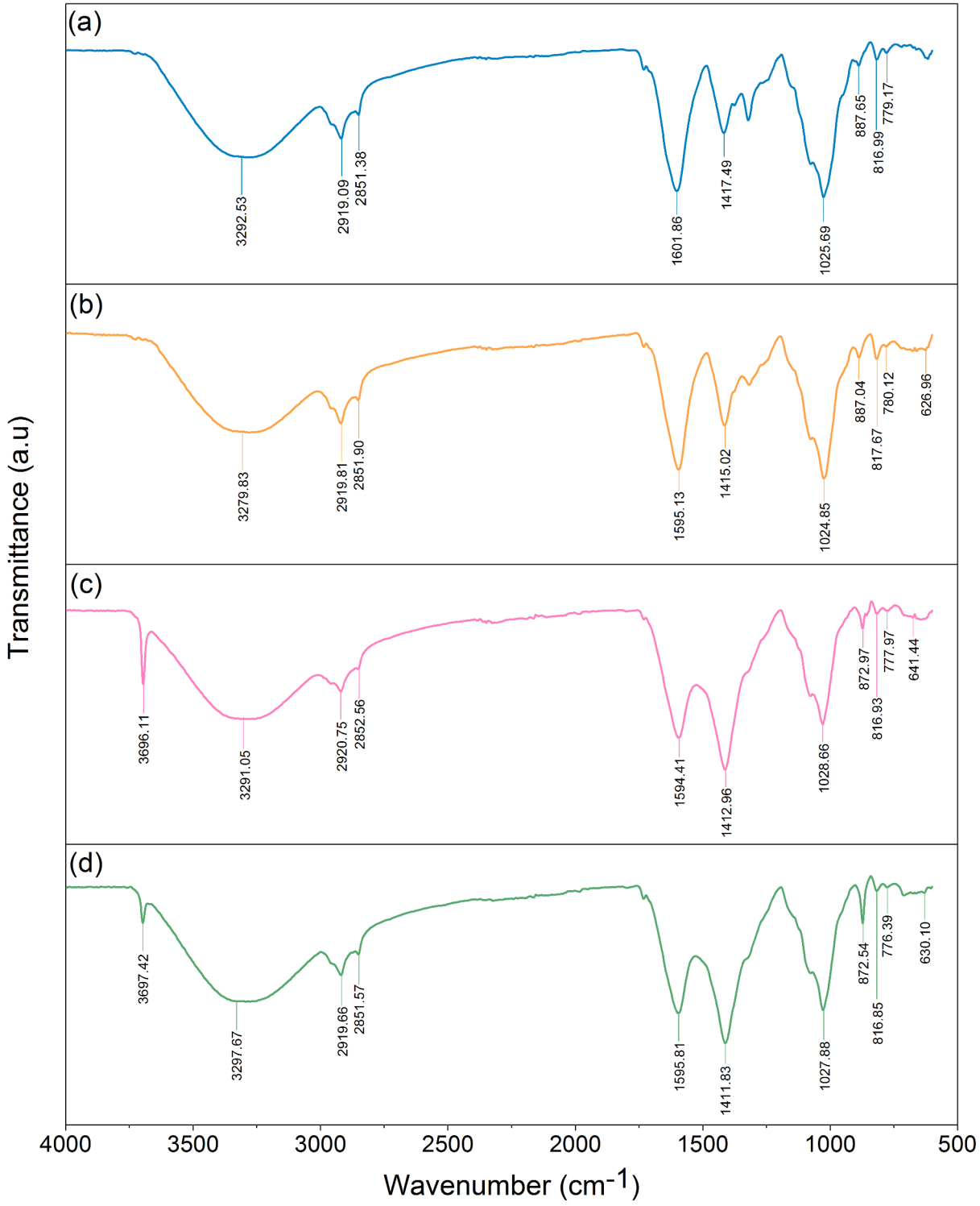

Fig. 5. FT-IR spectra of (a) BPB, (b) BPZB, (c) BPMB, and (d) BPZMB.

at 3600 cm^{-1} similar detected by previous studies that used MgO for modifying sugarcane bagasse and bagasse fly ash[41,42,48]. For C–H, it was C–H stretching vibration in cellulose presenting in a range of 2800–2900 cm^{-1} found in banana peels[49]. Moreover, the C–H stretching vibration in alkenes and aromatics was detected in a range of 700 cm^{-1} similar observed by the study of Akter, et al. used banana peels for removing dyes from textile effluent[50]. For C = O, it presented the carboxyl stretching vibration in carbohydrates and lignin found in a range of 1500–1600 cm^{-1}[50]. For C–O, it represented the carbonyl stretching vibrations of C–O–C of sodium alginate and cellulose at approximately 1020 cm^{-1} agreed with a previous study that used sodium alginate for synthesizing beaded materials from fruit peels[46]. In addition, it also referred to C–O of ester and ether in a range of 870–890 cm^{-1}[50]. For N–H, it was the deformation of amines at approximately 816 cm^{-1}[49].

The points of zero charge

The points of zero charge (pH_{pzc}) of BPB, BPZB, BPMB, and BPZMB were 5.37, 6.75, 9.87, and 9.43, respectively demonstrated in Fig. 6 which BPMB had a higher pH_{pzc} than other materials. Thus, the additions of MgO or ZnO increased the pH_{pzc} of materials, especially MgO similar found in previous studies that used MgO and ZnO for modifying sugarcane bagasse and bagasse fly ash for removing direct red 28 dye[41,42]. Moreover, the pH_{pzc}

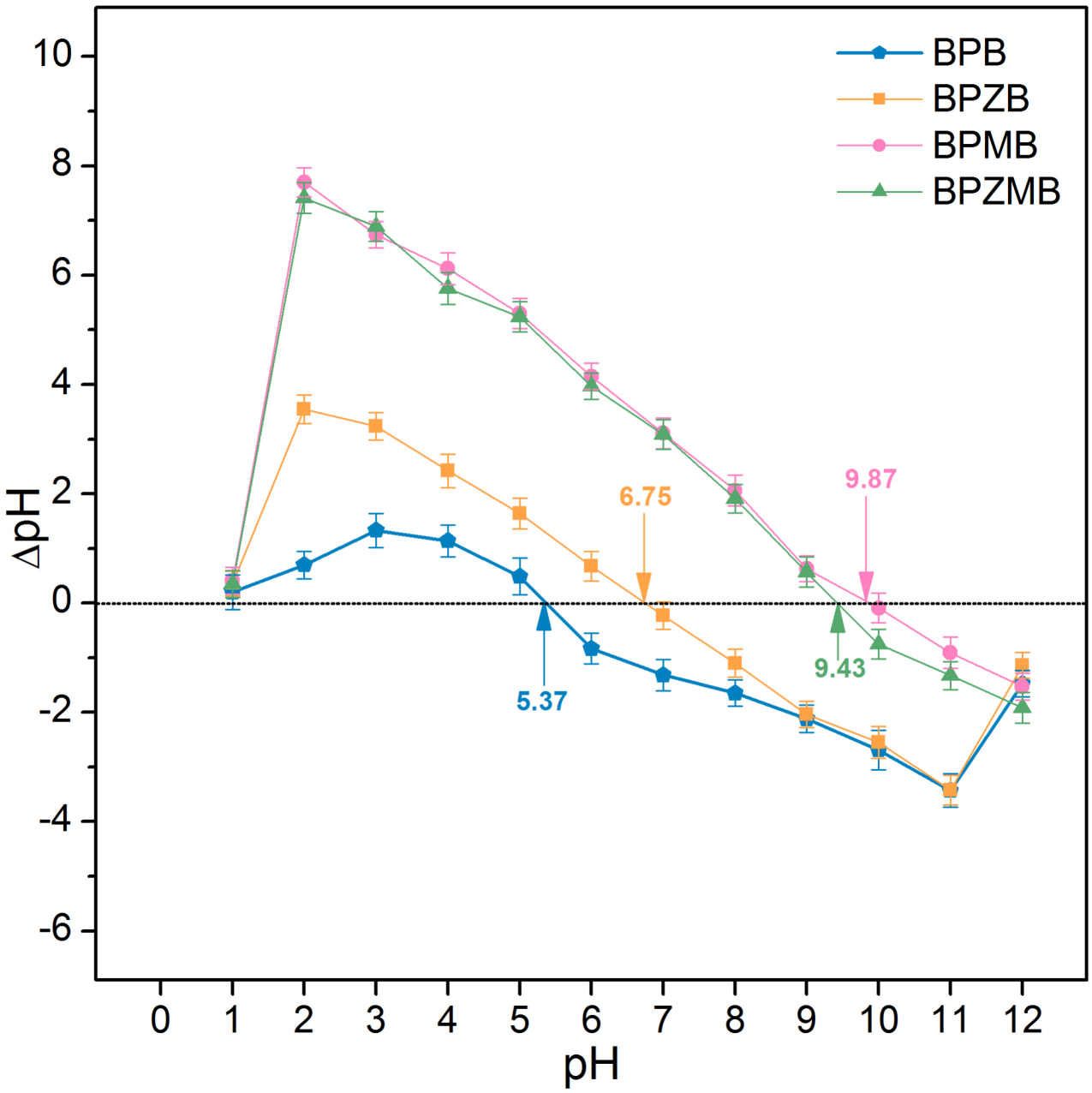

Fig. 6. The points of zero charge of BPB, BPZB, BPMB, and BPZMB.

values of BPMB and BPZMB were in an alkaline range similar to other studies reporting the pH_{pzc} of materials with adding MgO to be found in an alkaline range[42,48].

A series of batch experiments

Cadmium removal efficiencies by BPB, BPZB, BPMB, and BPZMB were investigated by a series of batch experiments. The results are demonstrated in Fig. 7a-f.

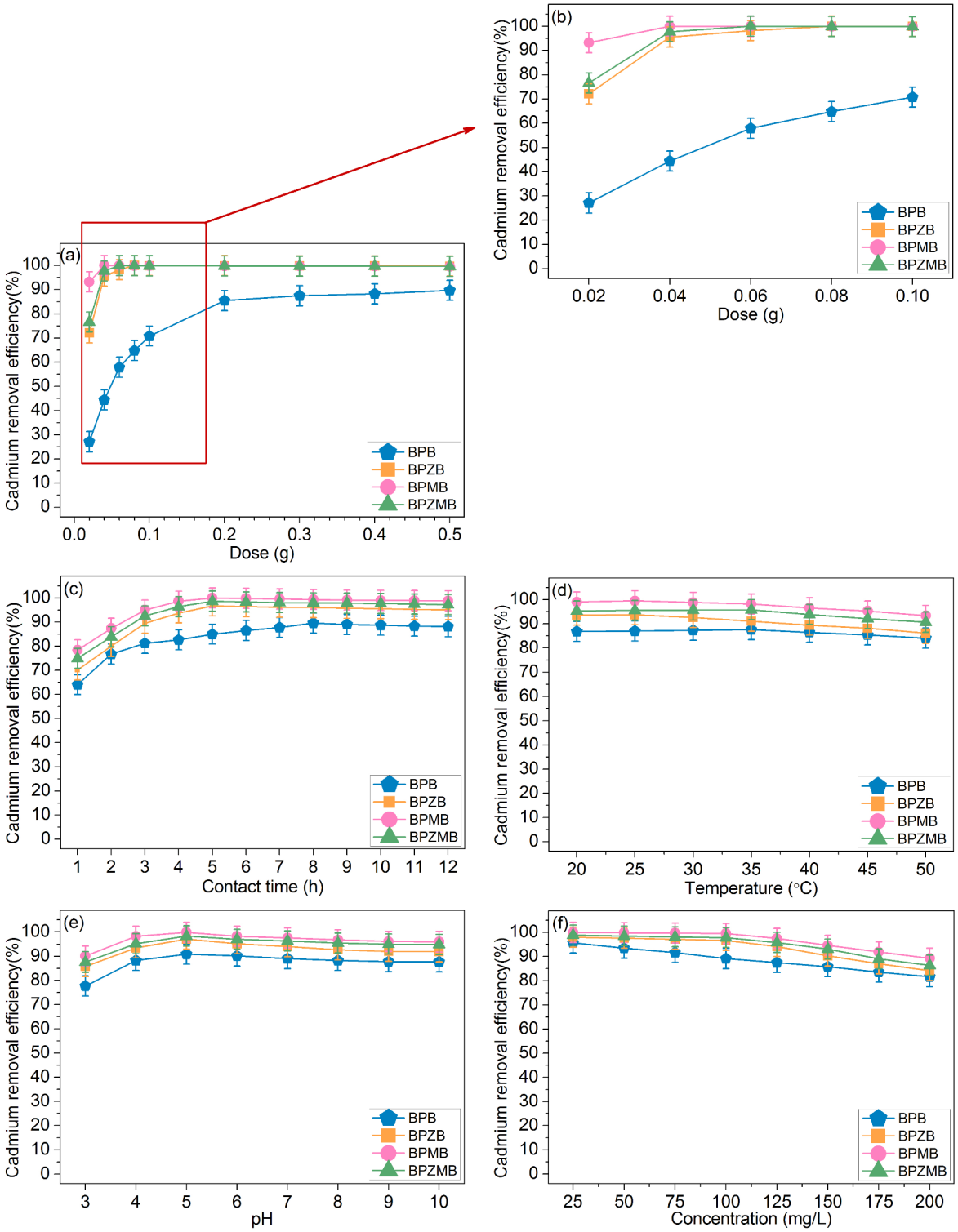

Fig. 7. Cadmium adsorptions by a series of batch experiments on the effects of (a and b) dose, (c) contact time (d) temperature, (e) pH, and (f) initial concentration of BPB, BPZB, BPMB, and BPZMB.

For the effect dose, the increase of material dosage resulted in the increase of cadmium removal efficiencies of BPB, BPZB, BPMB, and BPZMB from 0.02 to 0.2 g for BPB and from 0.02 to 0.08 g for BPZB, BPMB, and BPZMB, and then they were constant shown in Fig. 7a and b. The increase of material dosage increased the active site of material to capture cadmium(II) ions similar reported by the study of Ramutshatsha-Makhwedzha, et al. used activated carbon banana peels coated Al_2O_3-chitosan for removing lead and cadmium from wastewater[13]. The constant cadmium removal efficiency meant it went into the equilibrium of cadmium adsorption similar found by a previous study[13]. Moreover, the highest cadmium removal efficiencies of BPB, BPZB, BPMB, and BPZMB were found at 0.2 g for 85.50%, 0.08 g for 100%, 0.04 g for 100%, and 0.06 g for 100%, respectively, and they were used as the optimum material dosages in the contact time effect. Therefore, the addition of ZnO or MgO increased material efficiency by spending less adsorbent dosage than material without modification.

For the contact time effect, the cadmium removal efficiency of BPB was increased with increasing contact time from 1 to 8 h, whereas the cadmium removal efficiencies of BPZB, BPMB, and BPZMB were increased with increasing contact time from 1 to 5 h. The increase in contact time results in the increase of adsorption time between adsorbate on adsorbent. After that, they were constant which represented the saturated adsorption on adsorbent[20]. The results are demonstrated in Fig. 7c. The highest cadmium removal efficiency of BPB was found at 8 h for 89.54%, whereas the highest cadmium removal efficiencies of BPZB, BPMB, and BPZMB were found at 5 h at 96.69%, 100%, and 98.65%, respectively. The optimum material dosage and contact time of each material were applied to study the temperature effect. Therefore, the metal modifications by ZnO or MgO increased material efficiency by decreasing the adsorbent dosage and contact time for cadmium adsorption.

For temperature effect, the results are illustrated in Fig. 7d. The highest cadmium removal efficiencies of BPB and BPZMB were found at 35 °C for 87.63% and 95.85%, whereas the highest cadmium removal efficiencies of BPZB and BPMB were found at 25 °C for 93.81% and 99.53%. As a result, a temperature of 35 °C was chosen as the optimum temperature of BPB and BPZMB, and a temperature of 25 °C was chosen as the optimum temperature of BPZB and BPMB. The optimum material dosage, contact time, and temperature of each material were applied to study the pH effect.

For the pH effect, the reuslts are shown in Fig. 7e. The increase of pH affected the increase of cadmium removal efficiencies of BPB, BPZB, BPMB, and BPZMB from pH 3–5, and then they were stable which was similarly found in previous studies that the high cadmium adsorption at $pH > 5$[7,25]. In addition, the results also corresponded to their pH_{pzc} values were in a range of pH 5–10, so cadmium(II) ions could be adsorbed in those ranges while observing the stable cadmium removal efficiency. As a result, cadmium(II) ions could be adsorbed by all materials in a wide pH range from pH 5–10. Therefore, pH 5 was the optimum pH of all materials for obtaining the highest cadmium removal efficiency at 90.80%, 97.05%, 99.88%, and 98.34% for BPB, BPZB, BPMB, and BPZMB, respectively. The optimum material dosage, contact time, temperature, and pH of each material were applied to study the initial concentration effect.

For the initial concentration effect, the results are demonstreated in Fig. 7f. The increase of initial cadmium concentration from 25 to 200 mg/L resulted in the decrease of cadmium removal efficiencies of BPB, BPZB, BPMB, and BPZMB resulting from the decrease of the available adsorbent pore of material similar reported by previous studies[14,20]. For the initial cadmium concentration of 100 mg/L, the cadmium removal efficiencies of BPB, BPZB, BPMB, and BPZMB were 89.18%, 96.62%, 99.59%, and 97.85%, respectively.

In conclusion, the optimum conditions of material dosage, contact time, temperature, pH, and initial concentration of BPB, BPZB, BPMB, and BPZMB were 0.2 g, 8 h, 35 °C, pH 5, and 100 mg/L for 89.18%, 0.08 g, 5 h, 25 °C, pH 5, and 100 mg/L for 96.62%, 0.04 g, 5 h, 25 °C, pH 5, and 100 mg/L for 99.59%, and 0.06 g, 5 h, 35 °C, pH 5, and 100 mg/L for 97.85%, respectively which BPMB demonstrated a higher potential material than other materials because of spending less material dose than others with 99.59% cadmium removal efficiency. In addition, it could be arranged from high to low cadmium removal efficiency to be BPMB > BPZMB > BPZB > BPB. Therefore, the banana materials with ZnO or MgO modification increased material efficiency, especially MgO, and the material modification with ZnO and MgO in 50:50 ratios (BPZMB) illustrated a higher cadmium removal efficiency than banana material with or without ZnO modification.

Adsorption isotherms

The adsorption patterns of BPB, BPZB, BPMB, and BPZMB were investigated through the adsorption isotherms. Four isotherm models of Langmuir, Freundlich, Temkin, and Dubinin-Radushkevich in both linear and nonlinear models were used to determine which model was the better model to describe their adsorption patterns on cadmium adsorptions with choosing a high R^2 close to be 1.

Figure 8a-h demonstrated their plotting results, and Table 7 illustrated their adsorption isotherm parameters. Since R^2 values in linear and nonlinear Freundlich models of all materials were higher than other models, their adsorption patterns corresponded to the Freundlich model relating to a multilayer adsorption process. For the adsorption intensity (n), $1/n$ values in linear and nonlinear models of all materials were in a range of $0 < 1/n < 1$ which meant they favored cadmium adsorptions[21,44]. For the Freundlich constant (K_F), BPMB had a higher K_F value than other materials in both linear and nonlinear models, so it could strongly adsorb cadmium on BPMB.

The maximum adsorption capacity (q_m) comparison with previous studies that used banana peels for cadmium removal with or without modifications is demonstrated in Table 8. All materials in this study had higher q_m values than all previous studies in Table 8 except BPB had a lower q_m value than the study of Ge et al.[7] and Chen et al.[47]. Therefore, all materials in this study were potential materials for eliminating cadmium(II) ions in wastewater with the high q_m values especially BPMB demonstrated the highest q_m value of 454.55 mg/g than other materials. In the case of correct data translation, linear and nonlinear models are recommended to use for rechecking the correct results similar to other studies[48,44].

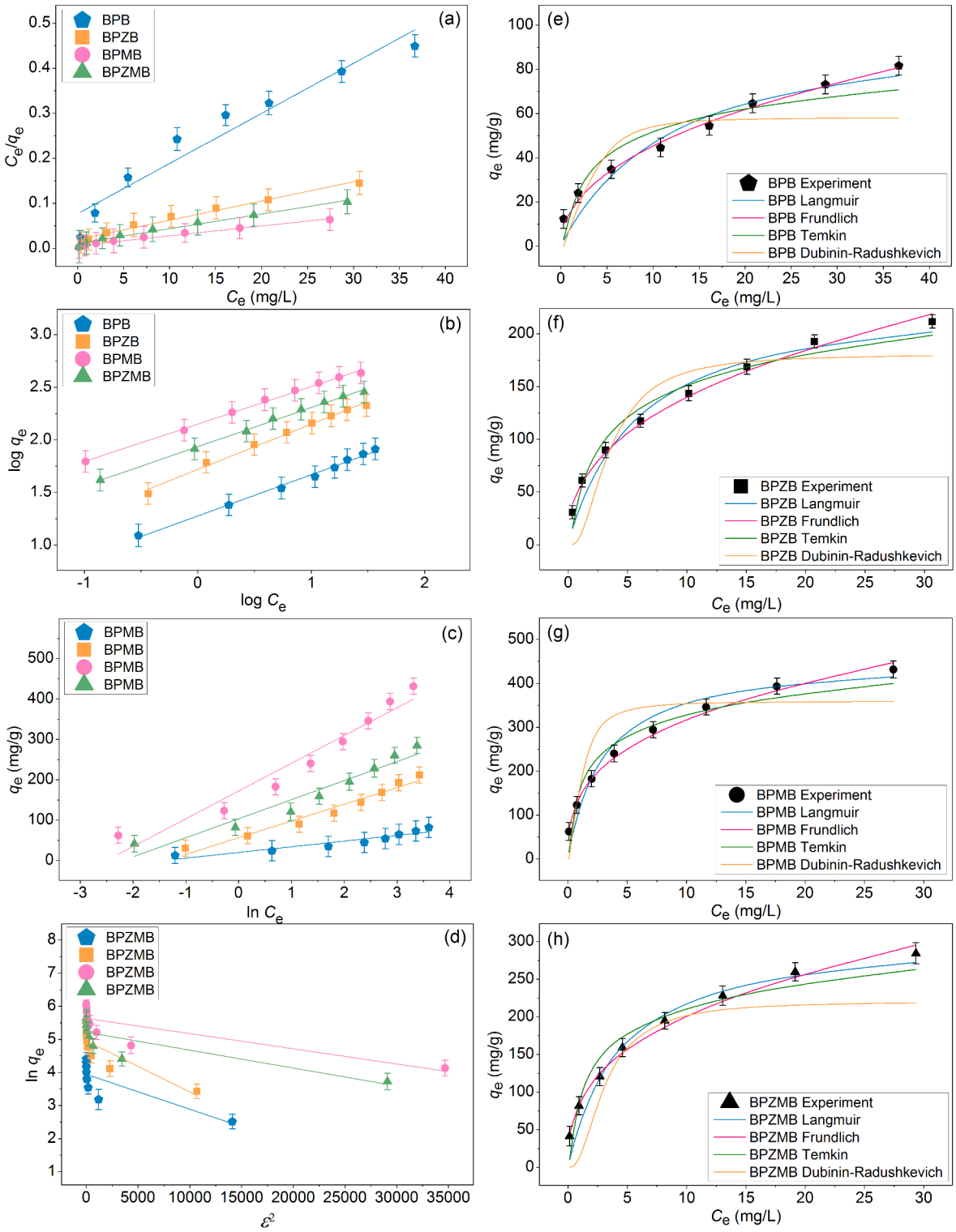

Fig. 8. Graphs of (a) linear Langmuir, (b) linear Freundlich, (c) linear Temkin, (d) linear Dubinin-Radushkevich, and nonlinear adsorption isotherms (e) BPB, (f) BPZB, (g) BPMB, and (h) BPZMB for cadmium adsorptions.

Adsorption kinetics

The adsorption rates and mechanisms of BPB, BPZB, BPMB, and BPZMB were investigated through the adsorption kinetics. Four kinetic models of pseudo-first-order kinetic, pseudo-second-order kinetic, Elovich, and intraparticle diffusion in both linear and nonlinear models were used to determine which model was better model to describe their adsorption rates and mechanisms on cadmium adsorptions with choosing a high R^2

Isotherm models	Parameters	BPB	BPZB	BPMB	BPZMB
Linear					
Langmuir	q_m (mg/g)	90.090	232.558	454.545	303.030
	K_L (L/mg)	0.144	0.218	0.386	0.314
	R^2	0.942	0.981	0.987	0.984
Freundlich	$1/n$	0.392	0.430	0.357	0.371
	K_F (mg/g)(L/mg)$^{1/n}$	18.919	52.336	141.873	86.080
	R^2	0.994	0.992	0.995	0.997
Temkin	b_T (J/mol)	182.035	59.963	36.006	54.293
	A_T (L/g)	4.158	3.939	12.360	8.980
	R^2	0.890	0.964	0.945	0.937
Dubinin-Radushkevich	q_m (mg/g)	51.578	141.599	279.807	183.993
	K_{DR} (mol^2/kJ^2)	0.0001	0.0002	0.0001	0.0001
	E (kJ/mol)	70.711	48.795	99.015	96.225
	R^2	0.664	0.761	0.702	0.694
Nonlinear					
Langmuir	q_m (mg/g)	92.176	236.959	455.978	310.480
	K_L (L/mg)	0.191	0.187	0.320	0.282
	R^2	0.937	0.967	0.985	0.981
	R^2_{adj}	0.926	0.962	0.983	0.978
	RMSE	6.572	12.519	31.206	17.994
Freundlich	$1/n$	0.408	0.393	0.334	0.352
	K_F (mg/g)(L/mg)$^{1/n}$	17.874	57.071	147.857	89.928
	R^2	0.994	0.995	0.994	0.993
	R^2_{adj}	0.993	0.994	0.993	0.992
	RMSE	2.039	5.008	11.065	7.685
Temkin	b_T (J/mol)	179.075	60.968	36.672	53.411
	A_T (L/g)	4.168	3.987	12.251	8.980
	R^2	0.890	0.964	0.942	0.937
	R^2_{adj}	0.871	0.958	0.932	0.926
	RMSE	8.686	13.145	34.020	23.418
Dubinin-Radushkevich	q_m (mg/g)	53.227	142.028	298.076	185.790
	K_{DR} (mol^2/kJ^2)	0.0001	0.0003	0.0002	0.0001
	E (kJ/mol)	78.069	44.518	47.613	96.903
	R^2	0.671	0.766	0.717	0.712
	R^2_{adj}	0.616	0.727	0.670	0.664
	RMSE	11.490	30.668	75.225	49.980

Table 7. Linear and nonlinear isotherm parameters for cadmium adsorptions on BPB, BPZB, BPMB, and BPZMB.

Adsorbents	Dose (g)	Time (min)	Temp. (°C)	pH	Conc. (mg/L)	Volume (mL)	q_m (mg/g)	References
Banana peel	0.04	1,440	-	6	3-150	40	12.39	[7]
Banana peel	0.125	30	25	6	5-100	20	44.00	[3]
Banana peel	0.1	840	25	5	25-1000	100	98.40	[47]
Banana peel (hydrochar at 200 °C)	0.125	30	25	6	5-100	20	4.20	[3]
Banana peel (hydrochar at 250 °C)	0.125	30	25	6	5-100	20	3.40	[3]
Banana peel (hydrocchar at 200 °C modified by Phosphoric acid (H_3PO_4))	0.04	1,440	-	6	3-150	40	94.52	[7]
Banana peel (Activated carbon coated with Al_2O_3)	0.1	40	25	6	20–100	20	43.00	[13]
BPB	0.2	480	35	5	25–200	100	90.09	This study
BPZB	0.08	300	25	5	25–200	100	232.56	This study
BPMB	0.04	300	25	5	25–200	100	454.55	This study
BPZMB	0.06	300	35	5	25–200	100	303.03	This study

Table 8. The maximum adsorption capacity of banana adsorbents for cadmium adsorption.

close to be 1. Similar to adsorption isotherms, the linear and nonlinear models were applied for rechecking the results.

Figure 9a-h demonstrated their plotting results, and Table 9 illustrated their adsorption kinetic parameters. The pseudo-second-order model was the best-fit model for all materials with a higher R^2 value than other kinetic models both in linear and nonlinear models, so their adsorption rates and mechanisms were a chemisorption

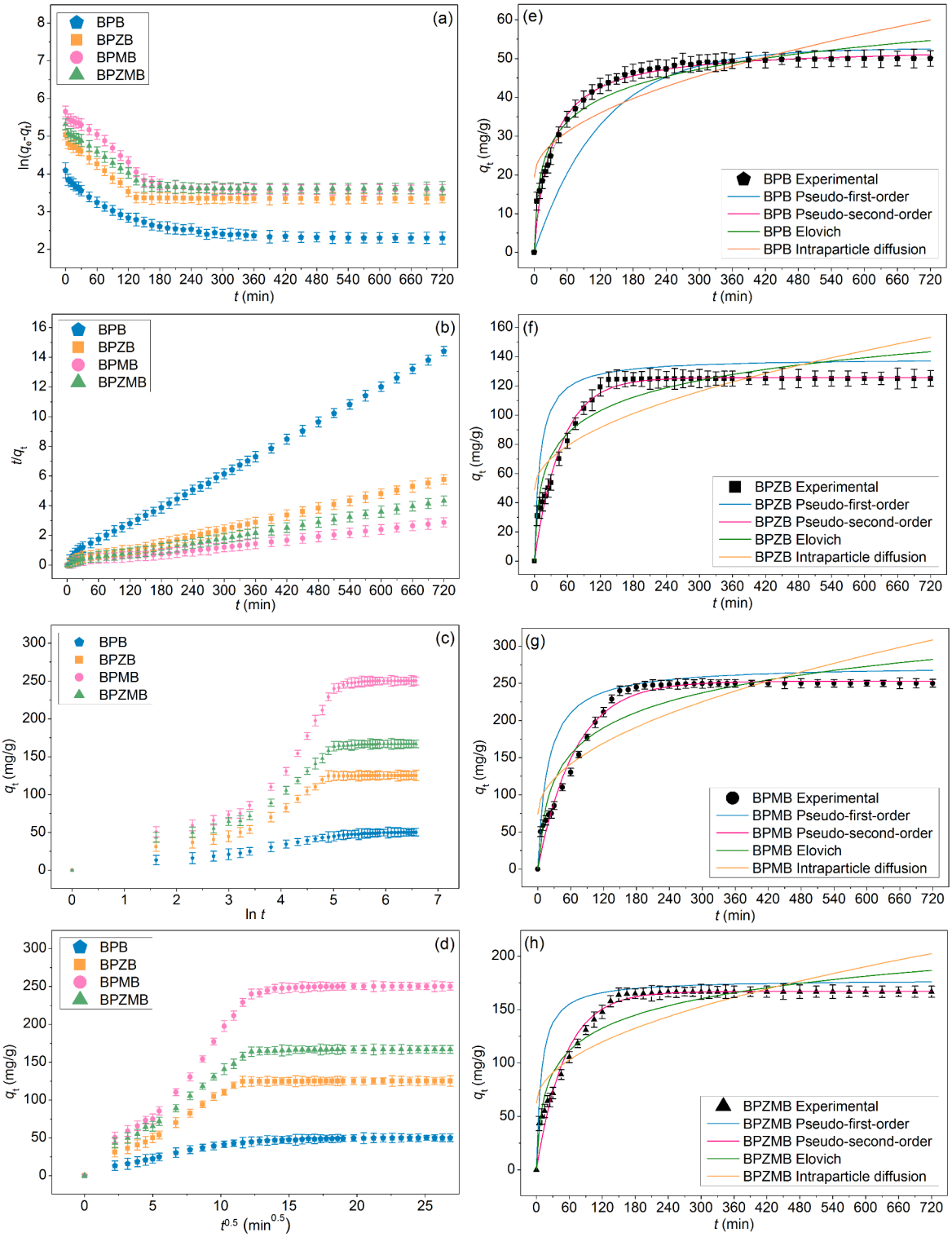

Fig. 9. Graphs of (a) linear pseudo-first-order, (b) linear pseudo-second-order, (c) linear Elovich (d) linear intraparticle diffusion, and nonlinear kinetic models of (e) BPB, (f) BPZB, (g) BPMB, and (h) BPZMB for cadmium adsorptions.

Kinetic models	Parameters	BPB	BPZB	BPMB	BPZMB
Linear					
Pseudo-first-order	q_e (mg/g)	27.311	65.157	124.188	89.918
	k_1 (1/min)	0.0020	0.0018	0.0026	0.0019
	R^2	0.660	0.491	0.586	0.536
Pseudo-second-order	q_e (mg/g)	52.083	129.870	270.270	175.439
	k_2 (g/mg·min)	0.0008	0.0015	0.0030	0.0020
	R^2	0.999	0.998	0.995	0.998
Elovich	α (mg/g·min)	1.000	1.000	1.000	1.000
	β (g/mg)	0.119	0.045	0.021	0.034
	R^2	0.957	0.896	0.901	0.913
Intraparticle diffusion	k_i (mg/g·min$^{0.5}$)	1.488	3.836	8.716	5.197
	C_i (mg/g)	19.376	48.711	73.841	62.567
	R^2	0.751	0.674	0.737	0.707
Nonlinear					
Pseudo-first-order	q_e (mg/g)	28.616	69.545	125.769	93.924
	k_1 (1/min)	0.0020	0.0021	0.0029	0.0019
	R^2	0.664	0.472	0.597	0.552
	R^2_{adj}	0.656	0.459	0.586	0.541
	RMSE	7.447	25.415	48.262	30.978
Pseudo-second-order	q_e (mg/g)	53.053	131.412	284.348	183.159
	k_2 (g/mg·min)	0.0006	0.0024	0.0040	0.0032
	R^2	0.992	0.992	0.993	0.992
	R^2_{adj}	0.991	0.991	0.992	0.991
	RMSE	1.237	8.652	14.695	25.816
Elovich	α (mg/g/min)	0.903	0.981	1.034	1.067
	β (g/mg)	0.144	0.053	0.029	0.038
	R^2	0.957	0.891	0.910	0.914
	R^2_{adj}	0.956	0.888	0.908	0.911
	RMSE	2.674	11.573	22.780	13.598
Intraparticle diffusion	k_i (mg/g·min$^{0.5}$)	1.510	3.885	8.744	5.206
	C_i (mg/g)	19.435	48.921	73.842	62.670
	R^2	0.750	0.673	0.737	0.706
	R^2_{adj}	0.744	0.664	0.731	0.699
	RMSE	6.426	20.016	38.947	25.074

Table 9. Linear and nonlinear kinetic parameters for cadmium adsorptions on BPB, BPZB, BPMB, and BPZMB.

process agreed with other previous studies[14,42]. The comparing cadmium adsorption capacity (q_e) and pseudo-second-order kinetic rate constant (k_2) in a pseudo-second-order model, BPMB had a higher both q_e and k_2 in both linear and nonlinear models than other materials, so it might be a higher cadmium adsorption with a fast adsorption rate than others. In addition, it could be a range from high to low of q_e and k_2 to be BPMB > BPZMB > BPZB > BPB. Moreover, the results also corresponded to batch tests that BPMB had higher cadmium adsorption than BPB, BPZB, and BPZMB.

Thermodynamic study

Since the changing temperature may affect to cadmium removal efficiency of materials, the thermodynamic study is used to investigate how it affects. The results are demonstrated in Table 10, and their thermodynamic plots for cadmium adsorptions are shown in Fig. 10a-d. The ΔG° values of all materials were negative which means their cadmium adsorptions could occur in a spontaneous nature, so the increase in temperature did not favor their cadmium adsorptions. In addition, their ΔH° were negative representing an exothermic process in nature. Since they were in a range of (-20) – (-80) kJ/mol, they were physical and chemical adsorption processes[31]. For ΔS°, they were negative which meant the decrease of the randomness during the adsorption process[44].

Material reusability

Before the materials are applied in industrial plants, it is necessary to test the efficiency of the material to see how many times it can be reused to be worth the investment through the desorption experiments. Three adsorption-desorption cycles were used for studying the material efficiencies of BPB, BPZB, BPMB, and BPZMB for cadmium removals, and their results are demonstrated in Fig. 11. Their cadmium removal efficiencies were

Temperature	ΔG° (kJ/mol)			
	BPB	BPZB	BPMB	BPZMB
293.15 K	-4.14	-7.53	-15.34	-10.19
298.15 K	-3.70	-7.16	-14.30	-9.87
303.15 K	-3.48	-7.02	-13.57	-9.42
308.15 K	-3.22	-6.67	-12.65	-9.05
313.15 K	-3.03	-6.45	-11.09	-8.72
318.15 K	-2.64	-6.15	-10.42	-8.24
323.15 K	-2.42	-5.72	-9.60	-7.98
ΔH° (kJ/mol)	-20.30	-24.27	-72.85	-32.40
ΔS°(J/mol K)	-55.37	-57.11	-196.04	-75.71

Table 10. Thermodynamic parameters of BPB, BPZB, BPMB, and BPZMB for cadmium adsorptions.

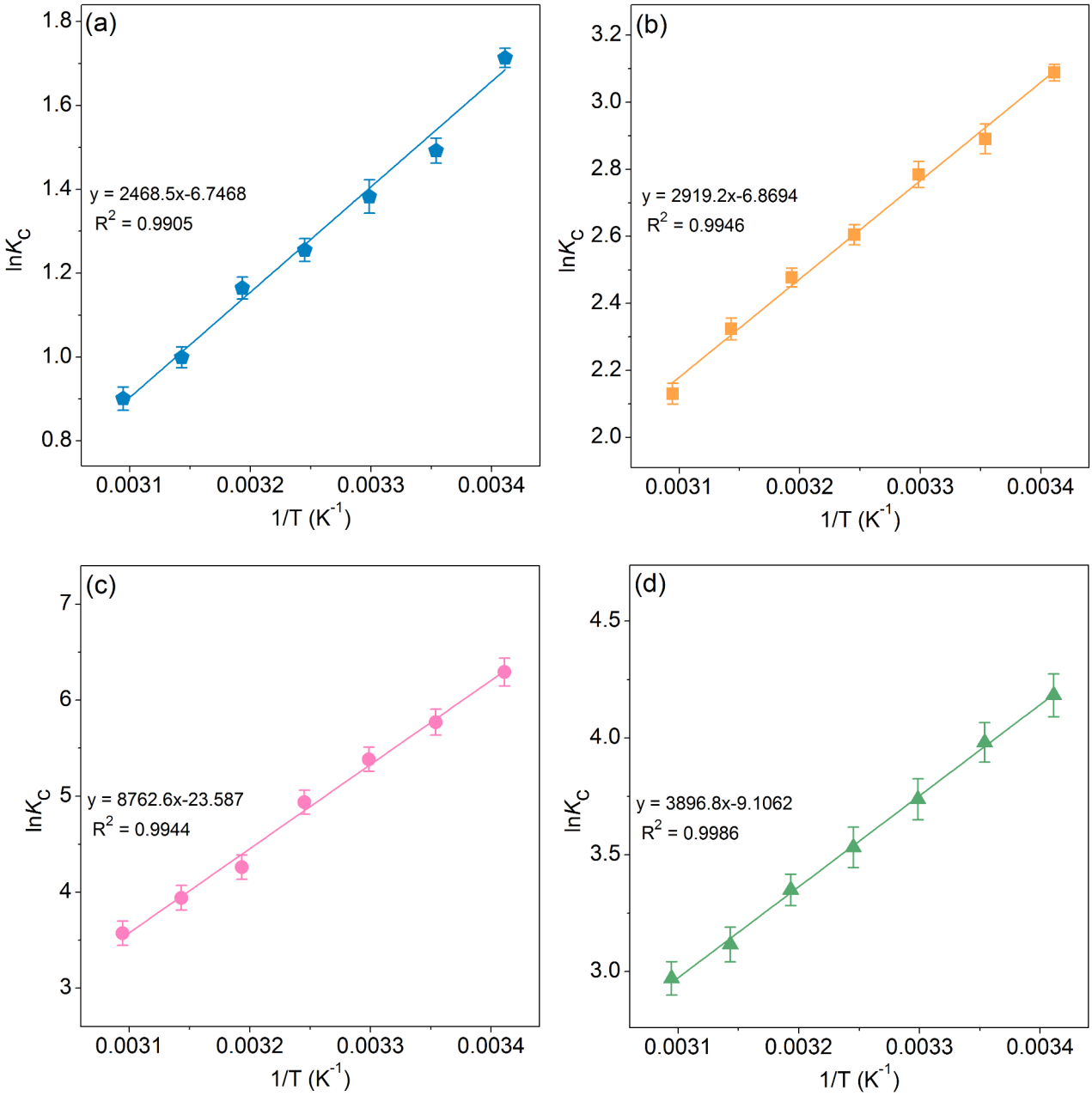

Fig. 10. Thermodynamic plots of (a) BPB, (b) BPZB, (c) BPMB, and (d) BPZMB for cadmium adsorptions.

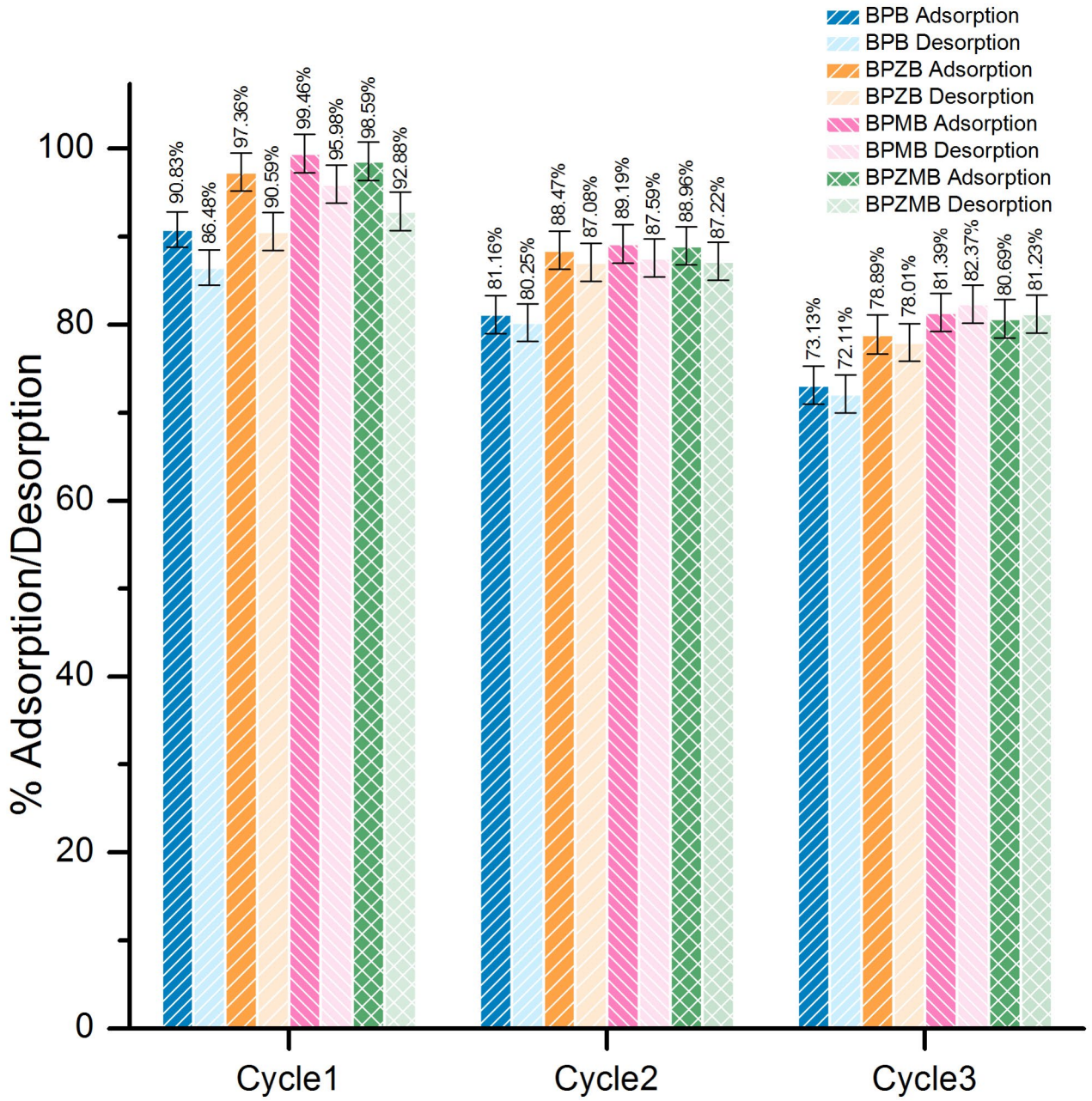

Fig. 11. Material reusability by desorption experiments of BPB, BPZB, BPMB, and BPZMB.

more than 73% after they were used in 3 cycles. Especially, BPMB had a cadmium removal efficiency of more than 81% after reusing 3 cycles. In addition, their cadmium removal efficiencies were approximately decreased by 10% for each cycle. Therefore, all materials are potentially applied in industrial wastewater treatment.

The possible mechanisms of cadmium adsorptions

The main possible process of electrostatic interaction could be used to explain adsorption mechanisms by BPB, BPZB, BPMB, and BPZMB which modified the idea from our previous study[24] are demonstrated in Fig. 12. Since banana peels composed of cellulose and lignin, they consisted of the hydroxyl group (–OH) which they could adsorb cadmium(II) ions through the electrostatic interaction by instead of the proton (H^+) by cadmium(II) ions. In addition, cadmium(II) ions are also adsorbed through the sharing electron of –OH and the complex compounds of banana peels and ZnO or MgO on the surface of BPZB, BPMB, and BPZMB through the electrostatic interaction.

The cost-effectiveness analysis

Before industrial uses, the cost-effectiveness analysis is an important issue in estimating whether a material is worth its use and investment. Generally, the choice of adsorbent is based on the availability of raw material,

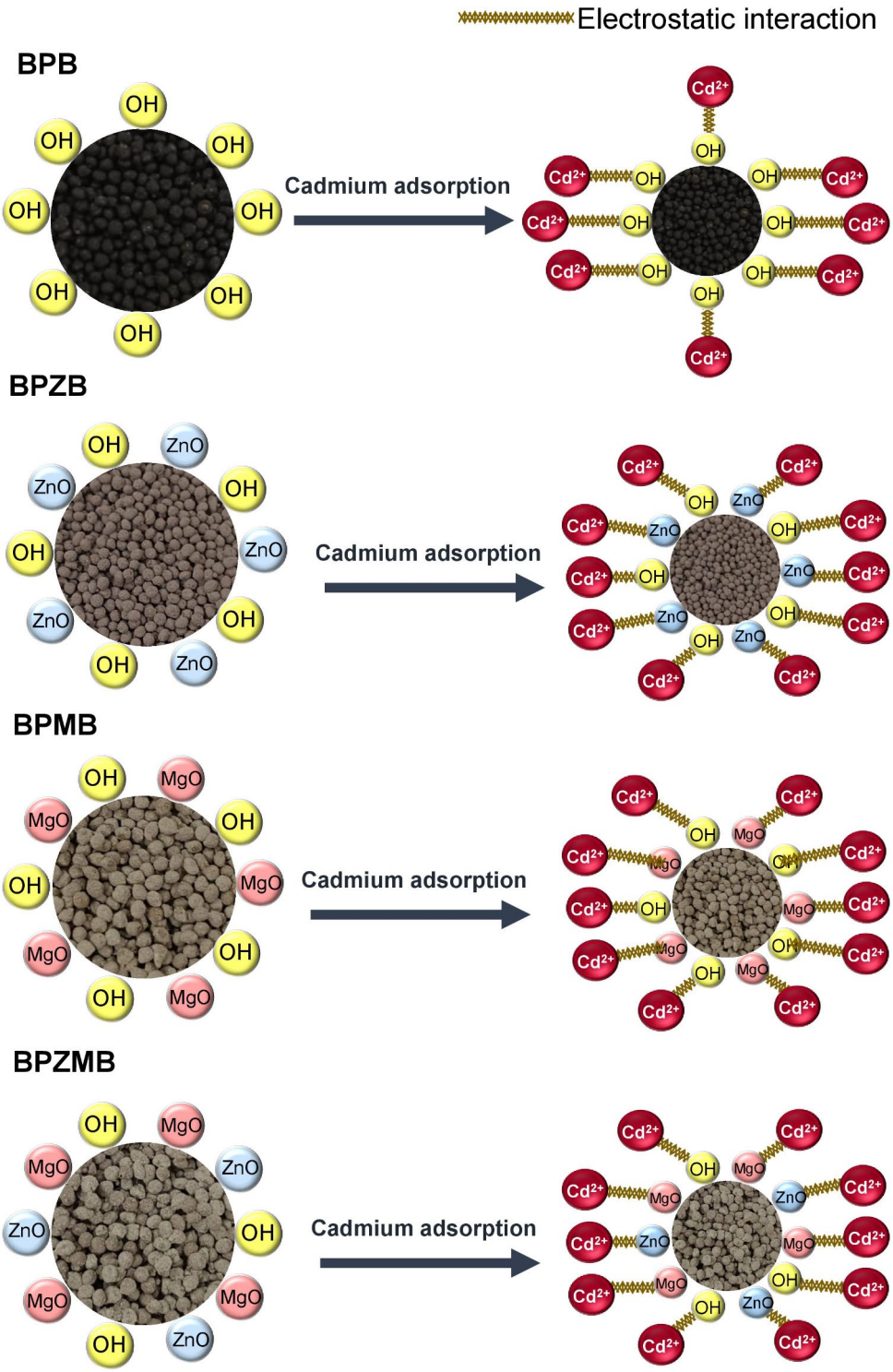

Fig. 12. Possible mechanisms of cadmium adsorptions by BPB, BPZB, BPMB, and BPZMB.

synthesis method, reusability, and usage. Since banana peels are waste, so there is no cost for raw materials. The chemical uses and synthesis methods of BPB, BPZB, BPMB, and BPZMB are suitable prices and simple synthesis steps. The material costs were approximately $20 per kg per material which referred from a previous study that used lemon peels for synthesizing beaded materials modified with ZnO or iron(III) oxide-hydroxide for reactive blue 4 dye removals[46]. Moreover, they could be reused in 3 cycles with a cadmium removal efficiency of more than 73%, so they helped to save an operation cost. Since they are beaded materials, they are easier to separate than powder materials. Therefore, they are good materials for adsorbing cadmium(II) ions for industrial applications.

Conclusion

- The novel cadmium adsorbents of banana powder beads (BPB), banana powder doped ZnO beads (BPZB), banana powder doped MgO beads (BPMB), and banana powder doped ZnO + MgO beads (BPZMB) were successfully synthesized by banana peels and two metal oxide of zinc and magnesium.
- The addition of ZnO or MgO into banana peels increased the specific surface area and pore volume of materials resulting in increasing the cadmium adsorption capacity of material, especially BPMB.
- XRD, EDX, and FT-IR techniques could confirm the ability of ZnO or MgO additions into BPZB or BPMB or BPZMB because they detected the specific peaks of ZnO or MgO, the chemical elements of zinc or magnesium, and the functional groups of Zn–O or Mg–O.
- The pH_{pzc} values of BPB, BPZB, BPMB, and BPZMB were 5.37, 6.75, 9.87, and 9.43, so ZnO and MgO increased the pH_{pzc} of material, especially MgO.
- BPMB demonstrated a higher cadmium removal efficiency of 99.59% than other materials with spending less material dosage than others. Therefore, the metal oxide helped to improve material efficiency, especially MgO.
- The maximum adsorption capacities (q_m) of BPB, BPZB, BPMB, and BPZMB were 90.09, 232.56, 454.55, and 303.03 mg/g which they had higher q_m values than other previous studies that used banana peels as raw material for adsorbing cadmium(II) ions in aqueous solution.
- They could be reused for more than 3 cycles with high cadmium adsorption of more than 73%.
- They were novel materials that used the simple step of material synthesis, suitable cost, easy use and separation after treatment, and capable of reusability responding to the worth use and investment. They also offered high performances for cadmium adsorption, so they were good choices of adsorbents for applying industry.

For future works, the continuous flow study should be investigated before being applied in industrial applications, and the competing anionic ions might be studied to confirm the specific target adsorption of materials. Moreover, real wastewater containing cadmium ions needs to be investigated to confirm their abilities for cadmium removal.

Data availability

The datasets used and/or analyzed during the current study are available from the corresponding author upon reasonable request.

Received: 8 July 2024; Accepted: 27 September 2024
Published online: 15 October 2024

References

1. Shrestha, R. et al. Technological trends in heavy metals removal from industrial wastewater: A review. *J. Environ. Chem. Eng.***9**, 105688 (2021).
2. Chen, Y. et al. Novel magnetic pomelo peel biochar for enhancing pb(II) and Cu(II) adsorption: Performance and mechanism. *Water Air Soil. Pollut.***231**, 404 (2020).
3. Yusuf, I. et al. Valorisation of banana peels by hydrothermal carbonisation: Potential use of the hydrochar and liquid by-product for water purification and energy conversion. *Bioresour. Technol. Rep.***12**, 100582 (2020).
4. Zhang, L. et al. Preparation of biochar by mango peel and its adsorption characteristics of cd(ii) in solution. *RSC Adv.***10**, 35878–35888 (2020).
5. Ahmadi, H. et al. Low cost biosorbent (Melon Peel) for effective removal of Cu(II), cd(II), and pb(II) ions from aqueous solution. *Case Stud. Chem. Environ. Eng.***6**, 100242 (2022).
6. Villen-Guzman, M. et al. Optimization of Ni(II) biosorption from aqueous solution on modified lemon peel. *Environ. Res.***179**, 108849 (2019).
7. Ge, Q., Tian, Q., Wang, S., Zhang, J. & Hou, R. Highly efficient removal of lead/cadmium by phosphoric acid-modified hydrochar prepared from fresh banana peels: Adsorption mechanisms and environmental application. *Langmuir*. **38**, 15394–15403 (2022).
8. Parlayici, Ş. & Pehlivan, E. Comparative study of cr(VI) removal by bio-waste adsorbents: Equilibrium, kinetics, and thermodynamic. *J. Anal. Sci. Technol.***10**, 15 (2019).
9. Poudel, B. R. et al. Agro-waste derived biomass impregnated with TiO_2 as a potential adsorbent for removal of as(III) from water. *Catalysts***10**, 1125 (2020).
10. Ramutshatsha-Makhwedzha, D., Mbaya, R. & Mavhungu, M. L. Application of activated carbon banana peel coated with Al2O3-chitosan for the adsorptive removal of lead and cadmium from wastewater. *Materials (Basel)***15**, 860 (2022).
11. Zhang, J. et al. Effects of excessive impregnation, magnesium content, and pyrolysis temperature on MgO-coated watermelon rind biochar and its lead removal capacity. *Environ. Res.***183**, 109152 (2020).
12. Hu, Z. T. et al. Banana peel biochar with nanoflake-assembled structure for cross contamination treatment in water: Interaction behaviors between lead and tetracycline. *Chem. Eng. J.***420**, 129807 (2021).
13. Ramutshatsha-Makhwedzha, D., Mbaya, R. & Mavhungu, M. L. Application of activated carbon banana peel coated with Al_2O_3-chitosan for the adsorptive removal of lead and cadmium from wastewater. *Materials (Basel)***15**, 860 (2022).
14. Praipipat, P., Ngamsurach, P., Kosumphan, S. & Mokkarat, J. Powdered and beaded sawdust materials modified iron(III) oxide–hydroxide for adsorption of lead(II) ion and reactive blue 4 dye. *Sci. Rep.***13**, 531 (2023).
15. Kalak, T., Kłopotek, A. & Cierpiszewski, R. Effective adsorption of lead ions using fly ash obtained in the novel circulating fluidized bed combustion technology. *Microchem J.***145**, 1011–1025 (2019).
16. Yang, T. et al. Enhancing cd(II) sorption by red mud with heat treatment: Performance and mechanisms of sorption. *J. Environ. Manag.***255**, 109866 (2020).
17. Pfeifer, A., Škerget, M. & Čolnik, M. Removal of iron, copper, and lead from aqueous solutions with zeolite, bentonite, and steel slag. *Sep. Sci. Technol.***56**, 2989–3000 (2021).
18. Praipipat, P., Ngamsurach, P. & Sanghuayprai, A. Modification of sugarcane bagasse with iron(III) oxide–hydroxide to improve its adsorption property for removing lead(II) ions. *Sci. Rep.***13**, 1467 (2023).
19. Ogata, F. et al. Wheat brans as waste biomass based on a potential bio–adsorbent for removing platinum(IV) ions from aqueous phase. *Bioresour. Technol. Rep.***20**, 101238 (2022).
20. Praipipat, P., Ngamsurach, P. & Pratumkaew, K. The synthesis, characterizations, and lead adsorption studies of chicken eggshell powder and chicken eggshell powder-doped iron(III) oxide-hydroxide. *Arab. J. Chem.***16**, 104640 (2023).

21. Praipipat, P., Ngamsurach, P. & Tannadee, R. Influence of duck eggshell powder modifications by the calcination process or addition of iron(III) oxide-hydroxide on lead removal efficiency. *Sci. Rep.***13**, 12100 (2023).
22. Castañeda-Figueredo, J. S., Torralba-Dotor, A. I., Pérez-Rodríguez, C. C., Moreno-Bedoya, A. M. & Mosquera-Vivas, C. S. Removal of lead and chromium from solution by organic peels: Effect of particle size and bio-adsorbent. *Heliyon***8**, e10275 (2022).
23. Threepanich, A. & Praipipat, P. Efficacy study of recycling materials by lemon peels as novel lead adsorbents with comparing of material form effects and possibility of continuous flow experiment. *Environ. Sci. Pollut Res.***29**, 46077–46090 (2022).
24. Praipipat, P., Ngamsurach, P. & Joraleeprasert, T. Synthesis, characterization and lead removal efficiency of orange peel powder and orange peel powder doped iron(III) oxide – hydroxide. *Sci. Rep.***13**, 10772 (2023).
25. Dinh, V. P. et al. Primary biosorption mechanism of lead(II) and cadmium(II) cations from aqueous solution by pomelo (*Citrus maxima*) fruit peels. *Environ. Sci. Pollut Res.***28**, 63504–63515 (2021).
26. Uche Augustine, A., Ishaq, B., Akpomie, T. M. & Odoh, R. Removal of lead(II) and iron(II) ions from aqueous solutions using watermelon (*Citrillus Lanatus*) peels as adsorbent. *Open. Access. J. Chem.***3**, 1–7 (2019).
27. Seleman, M. et al. Isotherms and kinetic studies of copper removal from textile wastewater and aqueous solution using powdered banana peel waste as an adsorbent in batch adsorption systems. *Int. J. Biomater.* 2012069 (2023). (2023).
28. Afolabi, F. O., Musonge, P. & Bakare, B. F. Bio-sorption of copper and lead ions in single and binary systems onto banana peels. *Cogent Eng.***8**, 1886730 (2021).
29. Bhagat, S., Gedam, V. V. & Pathak, P. Adsorption/desorption, kinetics and equilibrium studies for the uptake of Cu(II) and zn(II) onto banana peel. *Int. J. Chem. React. Eng.***18**, 20190109 (2020).
30. Praipipat, P., Ngamsurach, P., Bunchu, K., Lekwaree, V., Srirat, P., Chaiphumee, P., Noisri, J., and Aeamsa-ard, T. Comparative performance of fruit peel materials for methylene blue dye adsorption. *Int. J. Environ. Sci. Technol.* https://doi.org/10.1007/s13762-024-06037-1. (2024).
31. Praipipat, P., Ngamsurach, P., Srirat, P. & Chaiphumee, P. Engineered biosorbents of pomelo (*Citrus maxima* (Burm.f.) Merr) peels modified with zinc oxide and titanium dioxide for methylene blue dye sorption. *Sci. Rep.***14**, 5763 (2024).
32. Langmuir, I. The adsorption of gases on plane surfaces of glass, mica and platinum. *J. Am. Chem. Soc.***40**, 1361–1403 (1918).
33. Freundlich, H. Over the adsorption in solution. *J. Phys. Chem.***57**, 385–470 (1906).
34. Temkin, M. I. & Pyzhev, V. Kinetics of ammonia synthesis on promoted iron catalysts. *Acta Physiochim URSS***12**, 327–356 (1940).
35. Dubinin, M. M. & Radushkevich, L. V. The equation of the characteristic curve of activated charcoal. *Proc. USSR Acad. Sci.***55**, 327–329 (1947).
36. Lagergren, S. About the theory of so-called adsorption of soluble substances. *K Sven Vetenskapsakademiens Handl.***24**, 1–39 (1898).
37. Ho, Y. S. & McKay, G. Pseudo-second order model for sorption processes. *Process. Biochem.***34**, 451–465 (1999).
38. Elovich, S. Y. & Larinov, O. G. Theory of adsorption from solutions of non electrolytes on solid(I) equation adsorption from solutions and the analysis of its simplest form,(II) verification of the equation of adsorption isotherm from solutions. *Izv. Akad. Nauk. SSSR Otd Khim. Nauk.***2**, 209–216 (1962).
39. Weber, W. J. & Morris, J. C. Kinetics of adsorption carbon from solution. *J. Sanit. Eng. Div.***89**, 31–60 (1963).
40. MacQueen, J. T. Some observations concerning the van't hoff equation. *J. Chem. Educ.***44**, 755–756 (1967).
41. Praipipat, P. et al. Cationic oxides and dioxides of modified sugarcane bagasse beads with applications as low–cost sorbents for direct red 28 dye. *Sci. Rep.***14**, 1278 (2024).
42. Praipipat, P. et al. Synthesis and characterization of metal oxide dopped beaded sugarcane bagasse fly ash for direct red 28 dye removal. *J. Ind. Eng. Chem.***25**, 495–514 (2023).
43. Ngamsurach, P., Nemkhuntod, S., Chanaphan, P. & Praipipat, P. Modified beaded materials from recycled wastes of bagasse and bagasse fly ash with iron(III) oxide-hydroxide and zinc oxide for the removal of reactive blue 4 dye in aqueous solution. *ACS Omega***7**, 34839–34857 (2022).
44. Praipipat, P., Ngamsurach, P., Saekrathok, C. & Phomtai, S. Chicken and duck eggshell beads modified with iron(III) oxide-hydroxide and zinc oxide for reactive blue 4 dye removal. *Arab. J. Chem.***15**, 104291 (2022).
45. Shi, Q. et al. Efficient performance of magnesium oxide loaded biochar for the significant removal of Pb^{2+} and Cd^{2+}. *Ecotoxicol. Environ. Saf.***221**, 112426 (2021).
46. Praipipat, P., Ngamsurach, P. & Prasongdee, V. Comparative reactive blue 4 dye removal by lemon peel bead doping with iron(III) oxide-hydroxide and zinc oxide. *ACS Omega*. **7**, 41744–41758 (2022).
47. Chen, Y., Wang, H., Zhao, W. & Huang, S. Four different kinds of peels as adsorbents for the removal of cd(II) from aqueous solution: Kinetics, isotherm and mechanism. *J. Taiwan. Inst. Chem. Eng.***88**, 146–151 (2018).
48. Praipipat, P., Ngamsurach, P., Thanyahan, A. & Sakda, A. Reactive blue 4 adsorption efficiencies on bagasse and bagasse fly ash beads modified with titanium dioxide (TiO_2), magnesium oxide (MgO), and aluminum oxide (Al_2O_3). *Ind. Crop Prod.***191**, 115928 (2023).
49. Kamel, N. A., El-messieh, A., Saleh, N. M. & S. L. & Chitosan/banana peel powder nanocomposites for wound dressing application: Preparation and characterization. *Mater. Sci. Eng. C.* **72**, 543–550 (2017).
50. Akter, M., Rahman, F. B. A., Abedin, M. Z. & Kabir, S. M. F. Adsorption characteristics of banana peel in the removal of dyes from textile effluent. *Textiles***1**, 361–375 (2021).

Author contributions

P. P.: Supervision, Project administration, Conceptualization, Investigation, Methodology, Validation, Visualization, Writing - Original Draft, Writing-Review & Editing. P. N.: Visualization, Writing - Original Draft. Y. K.: Investigation. N. H.: Investigation.

Funding

This research received no external funding.

Declarations

Competing interests

The authors declare no competing interests.

Additional information

Supplementary Information The online version contains supplementary material available at https://doi.org/10.1038/s41598-024-74634-8.

Correspondence and requests for materials should be addressed to P.P.